Department of Biomedical Engineering

A Clinically Applicable Scaffold for Cardiac Regeneration

A Major Qualifying Project Report
Submitted to the Faculty of

WORCESTER POLYTECHNIC INSTITUTE
In partial fulfillment of the requirements for the
Degree of Bachelor Science

Submitted by:

Michael Fakharzadeh Gregory Fredette Emily Martin

Submitted to:

Advisor: Doctor Glenn Gaudette, Department of Biomedical Engineering

Project Code: GRG MQP 0802

Abstract

Myocardial infarction occurs when oxygen is depleted from cardiac muscle. Post myocardial infarction, the left ventricular wall is weakened due to the formation of scar tissue. As a result, a ventricular aneurysm may occur. There are numerous current treatment methods for ventricular aneurysms; however, none of them have been proven to promote cardiac regeneration. This project aims to find a method of reinforcing the weakened tissue and restoring normal cardiovascular function. A scaffold for cardiac regeneration will provide the long term reinforcement necessary to prevent ventricular aneurysms and restore normal heart function. Human mesenchymal stem cells (hMSCs) are commonly used because of their ability to differentiate into other cell types, including cardiac myocytes. This paper proposes a method of restoring cardiac tissue through the use of a novel implantation method using an hMSC seeded scaffold that will temporarily support the area of weakened tissue and aid in the production of cardiac myocytes to re-establish a healthy ventricular wall.

Executive Summary

Cardiovascular disease is the leading cause of death for both men and women in the United States .[1] The most common cause of cardiovascular disease is the narrowing or blockage of the coronary artery, which typically leads to a heart attack.[2] Annually in the United States, 1.2 million people suffer from heart attacks. Of those 1.2 million people, over 40% of them are suffering from a recurring heart attack.[3] After a heart attack, which is also known as myocardial infarction, the left ventricular wall is weakened due to the formation of scar tissue. This scar tissue has inferior mechanical properties when compared to normal myocardial tissue. As a result, a ventricular aneurysm may occur.

The two current surgical treatment methods for ventricular aneurysms are: direct linear closure and endoventricular patch plasty. Direct linear closure involves an excision of the scar tissue followed by reconstruction of the left ventricular wall in order to close the wound; endoventricular patch plasty involves excision of the scar tissue followed by replacement with a biomaterial patch.[4] Unfortunately, neither of these treatment methods replace healthy myocardium mechanically and biologically. This project aims to find a method of reinforcing the weakened tissue and restoring normal cardiovascular function. A scaffold for cardiac regeneration will provide the long term reinforcement necessary to prevent ventricular aneurysms and restore normal heart function. Human mesenchymal stem cells (hMSCs) are commonly used because of their ability to differentiate into other cell types, including cardiac myocytes. This paper proposes a method of restoring cardiac tissue through the use of a novel implantation method using an hMSC seeded scaffold that will temporarily support the area of weakened tissue and aid in the production of cardiac myocytes to re-establish a healthy ventricular wall.

Table of Contents

Authorship

Section	Author	Editor
Abstract	EM	MF
Executive Summary	EM	MF
Chapter 1: Introduction	EM	MF
Chapter 2: Background	-	-
2.1: Healthy Human Heart	EM	MF
2.2: Rodent Heart	EM	MF/GF
2.3: Myocardial Infarction	EM	MF/GF
2.4: Post-Myocardial Infarction	GF	MF/EM
2.5: Current Treatment Methods	EM	MF/GF
2.6: Cardiac Regeneration	-	-
2.6.1: Scaffolds	MF/GF	EM
2.6.2: Stem Cells	MF/GF	EM
2.6.3: Stem Cell Seeded Scaffolds	EM/MF	GF
2.6.4: Growth Factors	EM/MF/GF	EM
Chapter 3: Project Approach	-	-
3.1: Project Hypothesis	MF	EM
3.2: Project Assumptions	MF	EM
3.3: Project Goals	MF	EM
Chapter 4: Design	-	-
4.1: Stakeholders	GF	MF/EM
4.2: Objectives, Constraints, Functions	GF	MF/EM
4.3: Specifications	GF	MF/EM
4.4: Revised Client Statement	GF	MF/EM
4.5 Design Alternatives	GF	MF/EM
4.6 Final Design	GF	MF/EM
Chapter 5: Methodology	-	-
5.1: Fatigue Test Apparatus	EM	MF
5.2: Self-Sealing Test	EM	MF
5.3: Fatigue Strength Test	EM	MF
5.4: Quantum Dot Migration Test	EM	MF
5.5: *In Vivo* Test	EM	MF
Chapter 6: Results		
6.1: Self-Sealing Test	MF/EM	EM
6.2: Fatigue Strength Test	MF/EM	EM
6.3: Quantum Dot Migration Test	MF/EM	EM
6.4: In Vivo Test	EM	MF
Chapter 7: Analysis and Discussion	EM	MF
Chapter 8: Conclusion	GF	MF
Chapter 9: Future Recommendations	GF/MF	MF/EM

Table of Figures

Table of Tables

Chapter 1: Introduction

Cardiovascular disease is the leading cause of death for both men and women in the United States .[1] Every 34 seconds a person in the U.S. dies from cardiovascular disease, resulting in more than 2500 deaths each day.[4, 5] The most common cause of cardiovascular disease is the narrowing or blockage of the coronary artery, which typically leads to a heart attack.[2] Annually in the United States, 1.2 million people suffer from heart attacks. Of those 1.2 million people, over 40% of them are suffering from a recurring heart attack.[3] A heart attack occurs when the blood supply to the heart is blocked. This depletes the heart muscle of oxygen, and after only a few minutes, the tissue may be irreparably damaged. This is known as a myocardial infarction. Scar tissue typically forms over the damaged tissue; however, it does not regain full function. As a result, the cardiac output of the heart is significantly reduced and the strength of the tissue is diminished.

Thinning of the myocardial tissue may result in a ballooning effect which is known as a ventricular aneurysm. Depending on their size, aneurysms can be asymptomatic or fatal. The rupturing of a ventricular aneurysm causes an opening to form in the ventricular wall. This diminishes the ability of the ventricle to withstand pressure, rendering it inoperative. The probability of an aneurysm rupturing is a function of its size. Ventricular aneurysms also give rise to further complications such as blood clotting and arrhythmias.[6] Blood clots become more prevalent in patients with a ventricular aneurysm due to the decreased contractility of the ventricular wall. As a result, pooling of the blood may occur, which causes turbulent blood flow. Turbulent blood flow results in damage to the cells. The damaged cells initiate a clotting cascade. Ultimately, a fibrin mesh coagulates the cells and depending on the size, it may block the passage of blood through a vessel.[2] If blockage occurs in the coronary arteries, myocardial infarction may result.

Arrhythmias are abnormal heart rhythms caused by a disruption in the electrical system of the cardiac muscle.[2] If tissue damage occurs in an area responsible for propagating electrical pulse, it will cause a disruption that could affect the rhythm of the heart. Depending on the severity of the arrhythmia, a pacemaker may be necessary to control electrical impulses throughout the heart.

Blood clotting and arrhythmias, commonly caused by ventricular aneurysms, have many adverse effects on the heart. Due to the adverse affects that may arise from this disorder, it is necessary to find a method of reinforcing the weakened tissue and restoring normal cardiovascular function. A scaffold for cardiac regeneration will provide the long term reinforcement necessary to prevent ventricular aneurysms and restore normal heart function. This paper proposes a method of restoring cardiac tissue through the use of a human mesenchymal stem cell (hMSC) seeded scaffold that will temporarily support the area of weakened tissue and aid in the production of cardiac myocytes to re-establish a healthy ventricular wall.

Chapter 2: Background

2.1 Healthy Human Heart

The human heart is essentially the "central powerhouse" of the circulatory system. The heart is responsible for circulating blood throughout the body. The blood not only supplies oxygen and nutrients to the body's tissues and organs, but it also removes and transports waste to the kidneys, the liver, and the lungs. The heart contracts and relaxes in a beating rhythm about 100,000 times per day in order to circulate blood.[7] The anatomy of the heart and the flow of blood through it are shown below in figure 1.

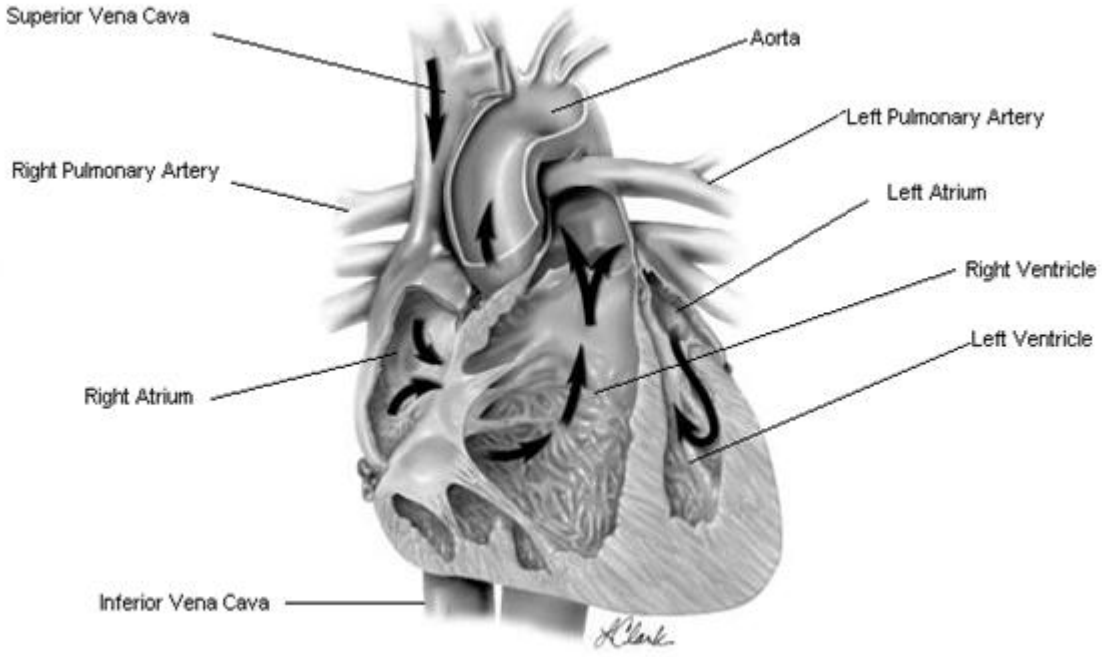

Figure 1: Cross Section of Human Heart[7]

Deoxygenated blood flows into the right atrium of the heart via the vena cava. It then passes through a tricuspid valve, which is a valve with three flaps, into the right ventricle. The right ventricle pumps the blood into the pulmonary artery, where it is taken to the lungs to become oxygenated. The oxygenated blood is taken away from the lungs and brought back to the left atrium of the heart via the pulmonary vein. The oxygenated blood passes through a bicuspid valve, which has two flaps, into the left ventricle where it is pumped into the aorta and taken throughout the body.[2]

The coronary arteries are the vessels that supply blood to the heart. Oxygenated blood leaves the left ventricle and passes through the aorta. The ascending aorta splits into two passage ways, one of which delivers the oxygenated blood to the left and right coronary arteries; the other leading to the aortic arch. The left coronary artery supplies blood to the left atrium and ventricle, while the right coronary artery supplies blood to the right atrium and ventricle. The coronary arteries run along the epicardium of the heart, supplying blood to the myocardium. Their role is vital in the nourishment of the myocardial tissue, since it is too thick to fully obtain nourishment from the blood passing through the chambers of the heart.[2]

The wall of the heart is composed of three layers: the epicardium, the myocardium, and the endocardium. The epicardium and the endocardium contain type I and type III collagen and elastin; in addition, the endocardium contains endothelial cells.[8, 9] The myocardium consists of cardiac muscle fibers, including fibroblasts and myocytes in a collagen matrix. These muscle fibers facilitate contraction of the heart via conduction of electric signals.[8, 10] The coronary arteries supply blood to the epicardium, the outermost layer, where it penetrates to the myocardium.[11] Therefore, when disruption of this blood flow occurs, damage or death to that particular region of the heart may occur.

2.2 Rodent Heart

The systemic and pulmonary circulation of a rodent heart is identical to that of a healthy human heart. As seen in Figure 2 below, the blood enters the heart at the right atrium via the vena cava.[12] It passes through a valve into the right ventricle then into the pulmonary artery. The pulmonary artery takes the deoxygenated blood to the lungs. From the lungs, the now oxygenated blood is taken to the left atrium via the pulmonary vein. From the left atrium, it enters the left ventricle, where it is pumped into the aorta and taken throughout the body.

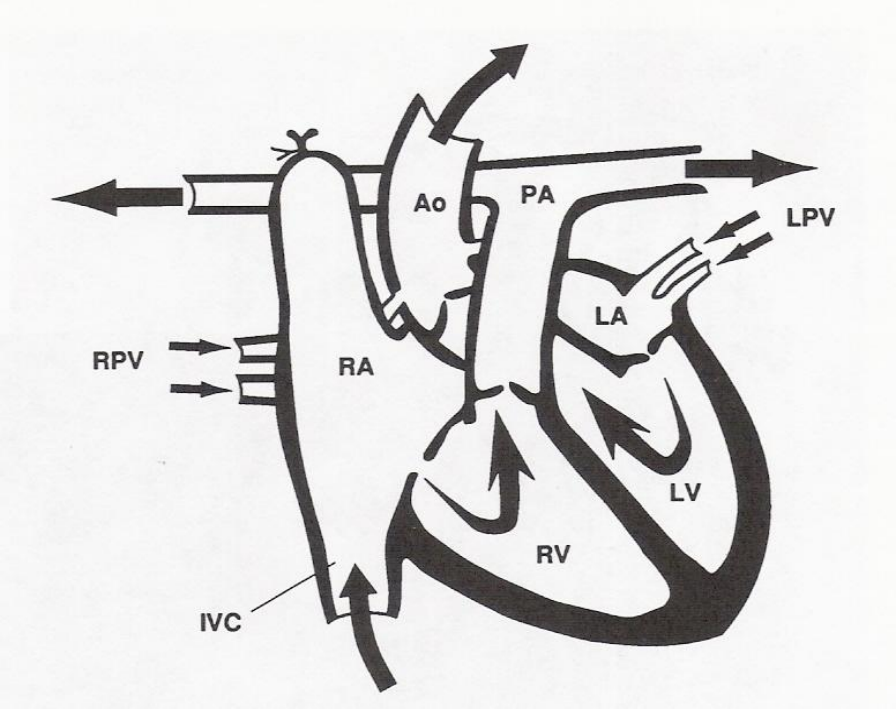

Figure 2: Blood Flow Through Rodent Heart[12]

The differences between the human heart and the rodent heart lie in the size, "the distribution coronary artery blood flow, dual blood supply in the rat to the right and left atrium of the heart, and heart to body weight ratios."[12] The average rodent heart beats at a rate of about 400 beats per minute, whereas a healthy human heart functions at about 70 beats per minute.[13] Despite these differences, the rodent heart serves as a favorable preliminary step in modeling the function of a scaffold for cardiac regeneration in the heart.

2.3 Myocardial Infarction

Coronary artery disease is one of several causes of a disruption of blood flow through the coronary arteries. A disruption in the blood flow may cause insufficient blood supply to the myocardium; this is also known as ischemia.[7] Ischemia occurs in three common ways: atherosclerosis, embolism, or artery spasm.[8, 14] Atherosclerosis is the congestion of the coronary artery as a result of plaque build-up on the vessel wall. Blockage of the coronary artery from the plaque may cause myocardial infarction. An arterial embolism is the blockage of an artery due to a blood clot.[15] When a blood clot blocks the coronary artery, it hinders blood flow to the heart,

preventing oxygen from reaching the myocardial tissue. An arterial spasm is a spasm of the arterial wall due to plaque build-up.[15] When this occurs in the coronary artery, the blood flow diminishes leading to a lack of oxygen supply to the tissue. In all the aforementioned cases, if the blood supply to the myocardium is blocked for more than a few minutes, it may cause damage or death to a portion of the tissue, also known as myocardial infarction.

Myocardial infarction, also known as a heart attack, occurs when blood supply to the myocardium is reduced or blocked due to congestion of one or more coronary arteries. Diminished blood flow, as a result of the blockage, reduces oxygen supply to the cardiac cells. Oxygen depletion greatly diminishes ATP production in the cells. A lack of ATP production results in reduced muscle contractility. If this persists for several minutes, tissue death occurs. In the weeks and month following tissue death, remodeling of the tissue occurs, resulting in scar tissue formation. The scar tissue primarily consists of fibroblasts and aligned fibrous collagen, which have inferior contractility to the native myocardium. These inferior properties are responsible for the formation of ventricular aneurysms.[16]

2.4 Post-Myocardial Infarction

Infarcted myocardium eventually develops into scar tissue. The scar tissue, which is mechanically unproductive, does not conduct the electrical charges that a healthy myocardium does. In fact, the scar tissue interrupts the normal charge pathways; therefore, the disrupted electrical pathways may result in arrhythmias, an abnormal beating of the heart. In addition, the heart does not produce the same output per contraction as it did prior to the occlusion. This also occurs due to a thinning of the ventricular wall at the site of the scar tissue. The increased pressure and thinning of the ventricular wall cause the heart to stray from its normal elliptical shape to a spherical shape, also known as a ballooning effect called ventricular aneurysms. Myocytes in the region try to compensate for the thinning and the reduced cardiac output by undergoing hypertrophy to increase healthy muscle mass.[17] As the heart muscle in the scarred region tries to compensate for its deficiencies, the stress on the heart increases. The extra muscle tissue produced by the myocytes amplifies the stress on the heart with each contraction. As a result, many complications may arise.

To treat, doctors use biomaterial scaffolds to provide extra support. These scaffolds provide mechanical support to the wall of the heart, which not only aid in maintaining the

elliptical shape, but also support the higher stresses exerted on the heart.[18] In patients with large scarring and left ventricular dysfunction, scaffolds have been shown to improve the overall heart function.[19]

Another side effect of infarction is congestive heart failure (CHF). If infarction significantly reduces cardiac output so much that systemic blood supply is insufficient, fluid build up, or edema, occurs. This condition is not acutely life threatening however, it causes shortness of breath which can limit physical activity.[6]

2.5 Current Treatment Methods

The two current treatment methods for ventricular aneurysms are: direct linear closure and endoventricular patch plasty. The direct linear closure procedure involves an excision of the scar tissue followed by reconstruction of the healthy tissue in order to close the wound. The advantage with this procedure is that there is a low probability of an inflammatory or an immune response occurring, since no biomaterials are used. The disadvantages associated with the direct linear closure procedure are: increased tension in the ventricular wall and the potential for a lack of tissue to facilitate wound closure.[20] The endoventricular patch plasty involves excision of the scar tissue followed by replacement with a biomaterial patch. The current gold standard material of choice is Dacron.[21] The advantages with this procedure are: potential reduction of ventricular wall tension, and revascularization and alignment of the muscle fibers.[20] The disadvantages with an endoventricular patch plasty are: the potential for an inflammatory or an immune response, and no cardiac regeneration.

2.6 Cardiac Regeneration

Cardiac patches are being researched as an important method of cardiac regeneration. Cardiac patches, or biomaterial scaffolds, are seeded with myocardial cells and implanted into the heart. The implanted scaffolds are being researched for their ability to stimulate regeneration of fully-functional myocardial cells that aid in the function of the heart.

Cardiac regeneration is a heavily debated topic among researchers. It was previously believed that myocardial cells terminally differentiate and do not divide in the adult heart. It was

also believed that the heart can only grow through myocyte hypertrophy.[22] However, recent studies have challenged this point of view, citing extra-cardiac cardiomyocytes growing in the hearts of several patients after cardiac transplants as evidence.[23]

The alternate point of view among researchers is that some myocardial cells divide. There is evidence that suggests that myocytes immediately express early and late growth-related genes after infarction.[24] These genes increase the number of dividing myocytes by a factor of 3 to 4, one week after infarction. The effects of this increase can be easily neglected since cell proliferation cannot occur where there is insufficient blood supply (i.e. the infarction site).[25] Since the infarction site is not ideal for cell proliferation, researchers have developed scaffolds that can be used to aid cardiac regeneration.

2.6.1 Scaffolds

Scaffolds are commonly used as a foundation of cardiac regeneration. Scaffolds are vital for sustained myocardial cell growth and general cardiac regeneration because they provide mechanical support for the cells until they form an extracellular matrix.[26] There are several varieties of scaffolds available, each with their strengths and weaknesses.

Park et al. developed a list of requirements that an ideal scaffold must meet:

> (1) Highly porous with large interconnected pores (to facilitate mass transport), (2) hydrophilic (to enhance cell attachment), (3) structurally stable (to withstand the shearing forces during bioreactor cultivation), (4) degradable (to provide ultimate biocompatibility of the tissue graft), and (5) elastic (to enable transmission of contractile forces).[27]

Dacron, a polyester mesh, is currently the gold-standard of treatment for endoventricular patch plasties. It has been used for its durability and flexibility.[28] However, Dacron has mechanical properties much higher than that of native myocardium, resulting in a material mismatch. In addition, it has been shown to induce thrombus formation.[29] While Dacron is a suitable material for a patch, it is not ideal for regeneration. Dacron does not resorb and it does not provide an ideal environment for cell survival and proliferation. In addition, it has been shown that Dacron is antigenic and induces an inflammatory response.[30] This creates an environment that is not conducive to cell survival and proliferation.

While Dacron patches are currently the gold-standard, Veritas is becoming a popular material choice for a scaffold to induce regeneration. Veritas is uncross-linked bovine pericardium. Veritas has been shown to resorb and promote tissue ingrowth and angiogenesis.[31]

Since vascularization is necessary for the survival of cells, this provides an ideal environment for cell viability and proliferation. Finally, the material has been shown to be biocompatible.[31] The pitfall of this material is that it is derived from bovine pericardium. While this material is advertised as mostly acellular, there is a potential for DNA extraction, which could elicit an immune response.

Porcine urinary bladder matrix (UBM) is currently being researched as a replacement for the non-degradable patches that are commonly used in clinical environments. The experiment which Robinson et al. conducted demonstrated that the replacement tissue consisted of characteristics of healing scarred and normal myocardium. Robinson et al.'s experiment also showed that only 10% of the UBM was remaining three months after implant [32]. Having degradation properties is advantageous for implantable scaffolds because they do not require a second surgery. However, if the degradation rate does not match the rate of regeneration problems may arise.

Fibrin glue is a common surgical sealant and adhesive that is composed of fibrinogen and thrombin.[33] Christman et al. concluded that transplanted cells are more likely to survive when injected in fibrin glue. However, fibrin glue does not have a positive effect on cell retention.[34]

2.6.2 Stem Cells

Stem cells are cells that have the ability to develop into various different cell types in the body. Currently, bone marrow is the most common source of cells for cardiac repair. The reasons for the use of bone marrow include: its ability to renew itself long-term and its ability to recompose a comprehensive array of progenitor cells after single-cell grafting.[35] Orlic et al. was able to promote myocardial regeneration in mice by injecting bone marrow cells into the infarction zone.[36] Potapova et al. was able to increase stroke work in canine hearts with defects by implanting bone marrow-derived stem cells.[37]

Human mesenchymal stem cells (hMSCs), which are derived from the bone marrow, are noted as having the ability to differentiate into cardiac myocytes, among other cell lines such as chondrocytes, osteocytes, and adipose cells.[38] Studies have shown that implantation of hMSCs in the scar tissue of the heart has improved heart function.[38] However, it is unknown whether this is due to cardiac myocyte proliferation or hMSC differentiation.

2.6.3 Stem Cell Seeded Scaffolds

Scaffolds are commonly used as a foundation of cardiac regeneration. Scaffolds are vital for sustained myocardial cell growth and general cardiac regeneration because they provide mechanical support for the cells until they form an extracellular matrix.[26] Park et al. developed a list of requirements that an ideal scaffold must meet. Some of these requirements include high porosity with interconnected pores to facilitate cell attachment and mass transport, a hydrophilic material to aid in cell attachment, and degradation properties for biocompatibility purposes.[27]

A scaffold that meets such requirements also needs to be seeded with stem cells to aid in some form of tissue regeneration. While cell density can be arbitrary, Table 1 summarizes some stem cell seeded scaffolds and the cell densities chosen by each group. This information will be valuable for determining the cell density that will be used for this design.

Type of cell	Cell Count	Scaffold	Reference
Myoblasts	80×10^6 cells/cm^2	Homologous acellular matrix	[39]
Bone marrow-derived mononuclear cells	8×10^6 cells/cm^2	PGCL polymer	[40]
Bone marrow MSCs	1×10^5 cells/cm^2	Bovine pericardium	[41]
Cardiomyocytes	6.67×10^5 cells/cm^2	3D collagen-based matrix	[42]

Table 1: Cellular Scaffold Seedings in Rodent Models

2.6.4 Growth Factors

Growth factors are another method of myocardial regeneration that has had some success. Vascular endothelial growth factor (VEGF) is commonly used in coalition with stem cells to promote cardiac regeneration. In order for cells to survive in the scar tissue, vascularization must occur. VEGF has been shown to stimulate endothelial cell proliferation, which results in angiogenesis. Angiogenesis is vital for the regeneration of myocardial tissue.[43] The use of growth factors appears to be a promising route as a method of promoting cardiac regeneration.

Matrix-metallo proteinases (MMPs) are enzymes that are involved in ventricular modeling through degradation of scar tissue.[44] Studies show that MMPs have an elevated concentration in the plasma of patients with congenital heart failure or ischemic tissue.[44] Finally, another study has shown that the ventricular dysfunction is lengthened when MMPs are inhibited.[44] This illustrates the importance of MMPs in the remodeling process, and as a result, consideration of MMP usage in scaffolds for cardiac regeneration is pertinent.

Chapter 3: Project Approach

3.1 Project Hypothesis

Unlike the current, conventional treatments of myocardial infarction, this project aims to develop a clinically applicable cardiac scaffold that actively seeks to regenerate cardiac tissue *in vivo*. It is hypothesized that the final scaffold design will regenerate cardiac tissue and restore myocardial function. The scaffold must be clinically viable, must have similar mechanical properties to the existing patches, must have regenerative properties, and must be successfully implanted into rats to meet this hypothesis.

3.2 Project Assumptions

There are assumptions that the group has made in order to allow this project to be completed within the time limits that are present. The problems of heart disease and myocardial infarction have been simplified in order to meet the required goals of this project in a timely manner. Some of the assumptions made by this project may not be accepted by every stakeholder; however, verifying these assumptions is well beyond the scope of this project. The following assumptions have been made:

- Following myocardial infarction, regeneration of the myocardium will improve cardiac function.
- Stem cells, specifically human mesenchymal stem cells, migrate to the infarction region and play an important role in myocardial regeneration.
- A fatigue testing apparatus can simulate the wear that a composite scaffold undergoes *in vivo*.
- Cell growth *in vitro* can model myocardial regeneration.
- Rats are an acceptable model for the human anatomy.

3.3 Project Goals

The purpose of this project was to develop and implant a scaffold that will regenerate cardiac tissue in the infarcted heart. The precise goals of this project are to:

- Develop a prototype scaffold that is cost effective, easily implantable, biocompatible, clinically applicable, and maintenance-less.
- Select suitable materials with the necessary mechanical and regenerative properties to support a section of the ventricular myocardium.
- Determine the mechanical properties of the candidate materials by testing them independently and in different combinations, with various procedures.
- Design a fatigue apparatus in order to test the fatigue properties of the candidate materials.
- Characterize the ability of the candidate materials to promote the viability and migration of human mesenchymal stem cells.
- Implant the selected scaffold in rodents in order to evaluate the effectiveness of the scaffold.

Chapter 4: Design

Professor Gaudette gave the group the following initial client statement for the project:

> *"Design a scaffold to promote cardiac regeneration for use in the surgical treatment of ventricular aneurysms. "*

Using this client statement, objectives, functions, constraints, and specifications were formed. Before such details could be defined, the stakeholders needed to be considered. Once the stakeholders and their needs were outlined, the group was able to follow the engineering design process to narrow the scope of the project. The objectives defined the final goals for the scaffold. The functions outlined the means the means that would be used in order to achieve the goals. The constraints limited the design space and the potential design options. Finally, the specifications set specific requirements for the design.

4.1 Stakeholders

Defining the stakeholders of the project was a crucial step in the design process. It allowed the group to determine who the scaffold was being designed for in order to deliver the most appropriate product. The main stakeholder is Professor Glenn Gaudette, who is an assistant professor of Biomedical Engineering at Worcester Polytechnic Institute. Professor Gaudette is an expert in the field of cardiac tissue engineering and his work is funded by the American Heart Association.

Another set of key stakeholders in this project are Dan Filipe and Megan Murphy. Both Dan and Megan are Biomedical Engineering graduate students at Worcester Polytechnic Institute. This project is largely based off of their study "*Design of a Composite Scaffold for Myocardial Regeneration Following Infarction"* which was completed in 2007.

The needs of Professor Gaudette are: to deliver a finished product by the final deadline of April 2008 and to fulfill the initial client statement. Also, Professor Gaudette is expecting a useful product with clinical applicability. Dan and Megan's needs are to continue their research, which is primarily based on the study that they began last year. Their research was primarily theoretical, while this project aims to take the results of their research and apply it practically.

Beyond the team of Professor Gaudette, Dan, and Megan, who are assisting the team on this project, two additional stakeholders are: the patients for whom the scaffold is being designed for and the cardiac surgeons who will be implanting them. It is imperative to consider the needs of these two parties. The patient's needs are: safety and usefulness (ideally the scaffold is implanted and regenerates lost cardiac myocytes without causing any adverse effects or harm). The cardiac surgeons need a product that is easy to implant as well as one that does not require pre-surgical preparation. In order to ensure that these needs are met, the team interviewed Adam Saltman M.D., Ph.D., the Director of Cardiothoracic Surgical Research at Maimonides Medical Center in Brooklyn, NY. Dr. Saltman has had experience with implanting both Urinary Bladder Matrix and Veritas in canine models. He indicated that Veritas was easy to work with and had the ability to self seal. In other words, once the Veritas was sutured into the heart, the material would seal around the sutures, which prevented blood leakage through the patch. This information was pertinent in the future consideration of Veritas as a scaffold candidate.

After considering the needs of all the stakeholders, the group considered their needs. This group needed to stay within the range of the time span and budget, while at the same time delivering a product that satisfied the needs of all the stakeholders. Once the group outlined all the needs of the stakeholders, the next step in the design process was to define the objectives, constraints, functions, and specifications. Those assisted in creating design alternatives as well as choosing a final design.

4.2 Objectives, Functions, Constraints

Defining a set of design objectives is a crucial part of the design process. It gives the designers a chance to think about what they want their design to do. Following much thought and brainstorming, the group formulated the following objectives for the composite scaffold.

Composite scaffold for cardiac cell regeneration

- The scaffold should be safe
  - Biocompatible material
  - Sterile
- The scaffold should be useful
  - The scaffold should regenerate cardiac cells

        - Promote cell viability
    - The scaffold should provide mechanical stability
        - Reliable mechanical properties
        - Prevent ballooning
    - The scaffold should be marketable
        - Reproducible
        - Easily implanted
        - Clinically viable

Above all, safety is the most important objective for the design. If the scaffold is not safe, then it is not practical for clinical applications. To ensure that the design is safe, it should be made of a biocompatible material. A biocompatible material is one can be implanted in the human body, and not be rejected by the organ on which it is implanted. The immune system is meant to protect the body from any foreign matter within the body. The material for the scaffold must be accepted by the immune system.

Beyond biocompatibility, the group also needed to consider the composite as a whole, specifically the effects that could arise when combining the various components. For the project the group will be combining stem cells and a scaffold material. Therefore, it is crucial that the union of these materials do not cause any unwanted reactions within the body. Finally, the scaffold must be sterile in order to protect patients from sustaining an infection due to implantation.

The next objectives include usefulness and practicality in the design. For this design, the scaffold should regenerate cardiac myocytes, provide mechanical stability, and be marketable. Based on the initial client statement the scaffold must promote cardiac regeneration. Cell viability must also be retained within the scaffold; at minimum the scaffold must foster an environment that maintains the initially seeded cells.

Mechanical stability is another aspect of usefulness that was considered. As previously indicated, ventricular aneurisms have a thinning effect on the ventricular wall due to the sub-par mechanical properties of the scar tissue. The scaffold design should have mechanical properties that resist the forces of the ventricular wall. These properties include: fatigue strength, stiffness, and tensile strength.

The last measure of usefulness is the scaffold's marketability. If the scaffold is too difficult to implant or manufacture, then its market value reduces. The scaffold should be made of a material with appropriate mechanical properties. Also, the scaffold should be reproducible, to ensure that market profits can maximized.

Using the design objectives, a weighted objective tree was made and can be found in Figure 3. The two main branches are safety and usefulness, which are weighted similarly. Both safety and usefulness are crucial to the successful design of an implantable scaffold. The sub-branches of safety include the material of the scaffold, its construction, and the sterility. Usefulness was sub-categorized by the ability to regenerate cardiac cells, the ability to provide mechanical support, and the scaffold's marketability. The weighted objective tree plays a role in elucidating the end goals of the project without extensively limiting the design space.

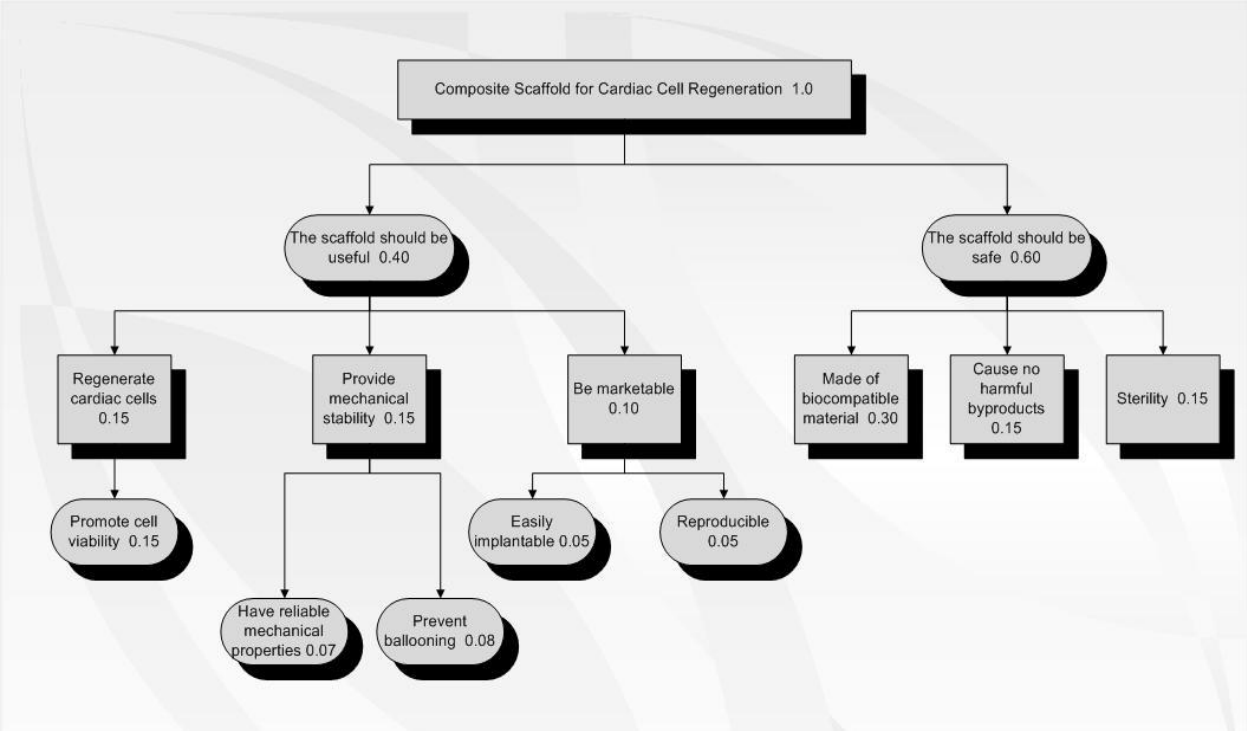

Figure 3: Weighted Objective Tree

The objectives provide the group with end goals; however, functions are necessary to characterize the design. Below is a list of the main functions that the cardiac scaffold must perform in order to meet the objectives:

Functions:

- Deliver stem cells
- Provide an environment for cells to thrive
- Facilitate surgical simplicity
- Provide mechanical stability
- Resist forces induced by heart
- Resist rubbing forces of the lungs

These functions assist in meeting the stated objectives. Additionally, these functions ensure that the final design is able to perform as requested in the design statement. Delivering stem cells is a function that must occur to allow the design to regenerate cardiac tissue. Seeding the scaffold improperly could result in cell loss or death which would prevent new tissue growth and promote design failure. Another point of possible failure with the stem cells is a lack of nourishment. It is imperative to successfully seed and deliver stem cells to the infarct region in order to ensure viability throughout the regenerative process.

The scaffold must meet required functions in order to prevent post infarction problems, such as aneurysms. The mechanical functions delineated, ensure that once implanted, the scaffold is able to prevent aneurysms and provide mechanical stability. As the heart beats, there are forces applied to the ventricular wall. Following infarction, there are weakened regions of the ventricular wall. The design needs to be able to handle those forces exerted by the ventricular wall. Due to the fact that the lungs and heart are so close, especially in a rodent model, the scaffold needs to be able to resist rubbing forces from the two organs. Lastly, to ensure that the needs of the surgeons are met, a necessary function of the scaffold was to facilitate surgical simplicity.

Since the group does not have unlimited time or funds to complete the research, the scope of the project was narrowed. In order to do that, the group compiled a set of constraints to limit the design space. The following constraints limit some options for design alternatives, while providing attainable goals for the project.

Constraints:

- Must be implantable

- Must be biocompatible
- Cannot cause harm to the user
- Must be durable
- Design costs cannot exceed the $468 budget
- Must be completed by April 2008

These constraints aid in narrowing the scope of the project, but they do not excessively limit potential solutions. The scaffold must be implantable and biocompatible. Following implantation the scaffold also needs to be biocompatible. Whenever implanting a material into the body, an immune response is elicited. This does not necessarily cause device failure, but it must be minimized. For this reason this device needs to be biocompatible, otherwise encapsulation may occur and cause device failure. In addition, release of any cytotoxic elements from the scaffold post-implantation could render the device unsafe for clinical use. The goal of this design is to regenerate lost tissue and heal an infarct site, not to harm the patient. Other important constraints that limit the design space are the budget and the time frame. This project must be completed within a year's time, on a budget of $468. These constraints allowed the design of the device to be completed within the allotted time and financial boundaries.

4.3 Specifications

The following specifications ensure that once implanted, the scaffold will be able to withstand the forces of the heart and prevent aneurysms. The scaffold must maintain at least the minimum mechanical integrity as defined by previous designs, in order to sustain forces on the ventricular wall. The scaffold should have a failure strength that is not statistically different before and after cyclic loading of 0.5Hz for 20,000 cycles at 120mmHg. "*Design of a Composite Scaffold for Myocardial Regeneration Following Infarction"* set standards for tensile strength and suture retention strength. However fatigue strength must also be tested due to the cyclic pressure loading on the ventricular wall.

4.4 Revised Client Statement

From the delineated objectives, functions, constraints, and specifications, the group was able to expand upon the initial client statement to provide a revised client statement, which includes all the key points of the project. The revised client statement is shown below:

Design an implantable scaffold to promote cardiac regeneration for use in the surgical treatment of ventricular aneurysms. The scaffold must maintain the minimum required mechanical properties as defined by previous designs. It must maintain its fatigue strength under conditions of at least 20,000 cycles at 0.5Hz under a pressure of 120mmHg. It must be clinically applicable, durable, and biocompatible. It must be safe for use in experimentation, be practical for surgical applications, have predictable biomaterial-tissue responses, and require minimal maintenance. The scaffold must withstand normal heart pressures, sustain normal heart function, facilitate surgical simplicity, and have the ability to self-seal. Finally, the design cannot exceed the budget of $468 and it must be completed by April 2008.

4.5 Design Alternatives

Based on the delineated objectives, functions, constraints, and specifications, design alternatives were formed. Originally two patch materials were selected, UBM and Veritas. A brainstorming session with Professor Gaudette, Megan Murphy, Dan Filipe, and the design team was held and a morphological chart was created (see Table 2). UBM and Veritas were chosen due to preliminary research done by Filipe et al. The suture retention strength and the tensile strength were previously characterized for these biomaterials. They were determined by Filipe et al. as good biomaterial candidates for cardiac regeneration. In addition, Filipe et al. determined that fibrin gel was a good host environment for hMSCs. Therefore, fibrin gel was used as a potential means to provide a conducive environment for cell growth. Collagen gel and the "microfracture" technique were ideas presented during a brainstorming session. Collagen gel seemed promising as a host environment for the cells since it is an abundant ECM protein. The "microfracture" technique offered a unique method of nourishing cells with blood flow. hMSCs were chosen to promote cardiac regeneration due to the abundance of studies that show their capabilities to differentiate into cardiac myocytes. VEGF and MMPs were considered in order to enhance cell function and to encourage new tissue formation. Due to budget constraints, VEGF and MMPs were not included in any of the design alternatives.

Table 2: Morphological Chart

Function	Means				
Maintain similar mechanical properties to a healthy rodent heart	UBM	Veritas			
Provide an environment conducive to cell growth	Fibrin Gel	Collagen Gel	"Microfracture" in scar tissue		
Promote cardiac Myocyte regeneration	hMSC's	hMSCs and VEGF	hMSCs and MMPs	hMSCs, VEGF, and MMPs	

Using this chart and ideas from the brainstorming session a set of five design alternatives were recorded.

- Scaffold seeded with hMSCs and punctured
- Scaffold seeded with hMSCs
- Two scaffolds with fibrin-seeded gel in between
- Scaffold with fibrin gel on top sealed with fibrin glue
- Scaffold injected with hMSCs

The first design involves a scaffold with seeded hMSCs that is implanted onto the heart. After implantation blood channels are opened up to provide cell nourishment. The second design is a scaffold that is seeded with hMSCs on one side. The scaffold would be prepared for a given time prior to implantation to allow cell migration into the patch. The third design uses two scaffolds with a fibrin gel solution containing the hMSCs in between. The two scaffolds would be sutured together to hold in the gel, then sutured onto the ventricular wall. The fourth design uses a scaffold and fibrin gel. In this design, the gel is placed on the scaffold and then fibrin glue is used to seal the gel. The scaffold would then be implanted facing down. The fifth design is a scaffold that is injected with hMSCs and implanted onto the ventricular wall.

Using the objectives, functions, and constraints a set of comparison objectives was created to compare the design alternatives. The five designs were then compared using a pairwise comparison chart (see Table 3). For each objective, each design was rated from 4 to 1, four being the best and one being the worst. After comparing all categories, the numbers for each design were tallied up and the design with the most points was chosen as the final design.

Table 3: Pairwise Comparison Chart

	Design			
Objectives	Scaffold seeded with punctures	Scaffold-fibrin gel -scaffold	Scaffold-fibrin gel –fibrin glue	Scaffold injected with fibrin gel
Safety	4	3	3	1
Delivery of cells	4	2	2	3
Promote cell viability	4	3	2	1
Manufacturability	3	2	4	1
Surgical simplicity	4	3	2	1
Cost	4	1	2	3
Biocompatibility	4	2	1	3
Totals	27	16	16	13

4.6 Final Design

Based on research, objectives, functions, constraints, specifications, and comparison by the pairwise comparison chart, a final design was chosen (see Figure 4). This final design incorporates a scaffold seeded with hMSCs followed by syringe needle punctures to the scaffold and through the ventricular wall. For this design, no scar tissue is excised from the infarcted region. The scaffold is seeded with hMSCs for a given amount of time pre-implantation is implanted on top of the scar tissue. This time will be determined via a cell loading assay.

This design is advantageous due to its simplicity. It is a clinically viable design that will be easy to surgically implant, since it only involves one component: the scaffold. Implanting the scaffold will require the same surgical technique as the implantation of any acellular patch used in the endoventricular patch plasty procedure; however, it also provides regenerative capability with the use of hMSCs. In addition, it is one of the safest design alternatives due to its surgical ease. Furthermore, the design is cost effective as a result of its simplicity. Finally, the needle puncture design allows for sufficient cell delivery and nourishment, to promote differentiation

and proliferation of cardiac cells. Overall, this design rated better than the others and was chosen to be the final design.

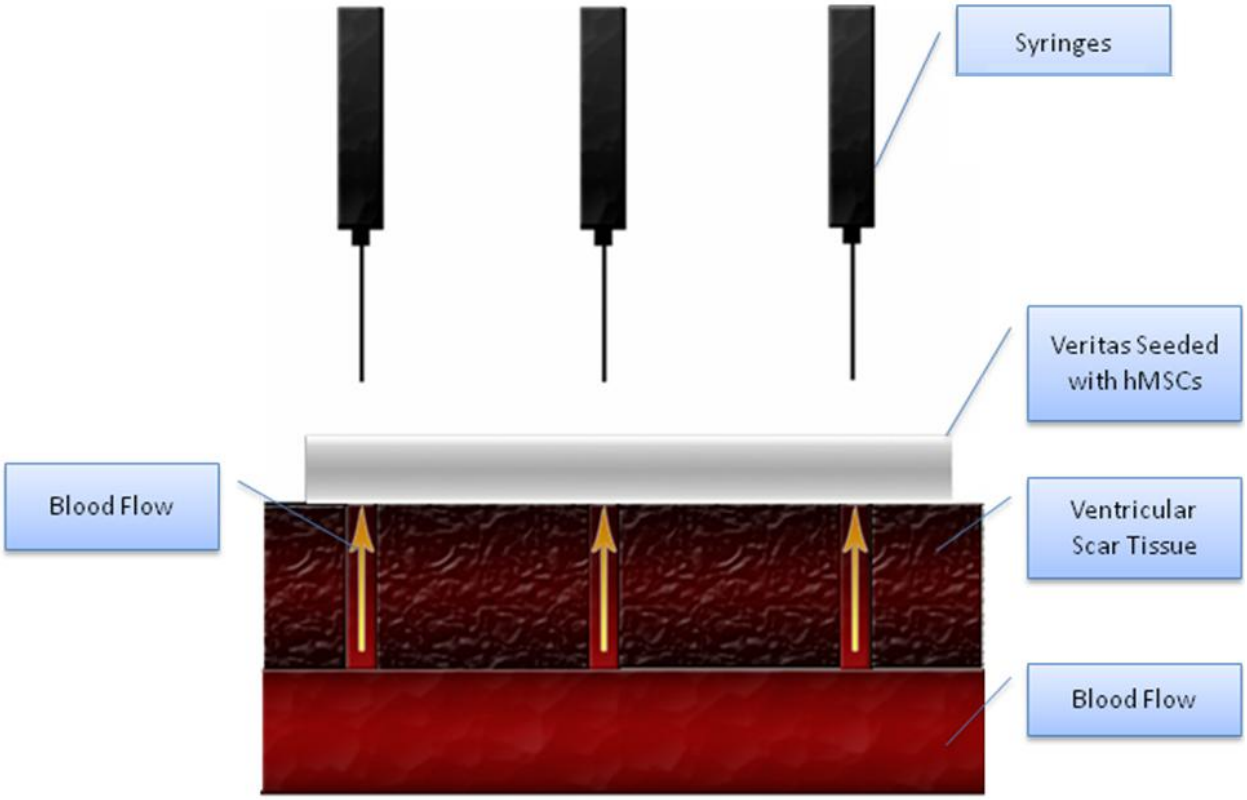

Figure 4: Final Design Schematic

Chapter 5: Methodology

In order to evaluate the design alternatives, it was necessary to conduct a series of tests to ensure that the scaffold met the specific aims of the project. As a continuation of a previous project, "*Design of a Composite Scaffold for Myocardial Regeneration Following Infarction,"* which validated the efficacy of bovine urinary bladder matrix (UBM) and bovine pericardium-derived collagen matrix (Veritas) for tensile and suture retention strength, it was essential to measure the fatigue properties of the two biomaterial considerations: UBM and Veritas. The specifications of the biomaterial scaffold are: the scaffold must maintain at least the minimum mechanical integrity as defined by previous designs, and the scaffold should have a failure strength that is not statistically different before and after cyclic loading of at least 20,000 cycles at 0.5Hz under a pressure of 120mmHg. In order to test the fatigue strength, it was necessary to design and build a fatigue test apparatus.

5.1 Fatigue Test Apparatus

The first step in designing the fatigue apparatus was to set specifications, objectives, constraints, and functions. The specification was: it must cyclically infuse and withdraw saline at a minimum rate of 0.5Hz at a pressure of 120mmHg for 12 hours. The objectives were: to run multiple tests at one time, to provide a uniform pressure which resulted in a ballooning effect on the scaffold, to measure both the pressure and the change in height via pressure transducers and a sonomicrometer, and to have a continuous system that could run for a 12 hour period. The constraints were: it must be sealed to prevent water leakage, it must be able to fasten the membranes, it must be able to infuse and withdraw saline at the rate indicated by the specifications, and it must maintain a minimum cyclic load of 120mmHg over the 12 hour period. The function was to provide a hydrostatic pressure on the scaffold, forcing it to balloon out in a repetitive nature, as a simulation of the forces experienced *in vivo* to ensure that the biomaterial has the necessary fatigue properties for *in vivo* applications.

After delineating the requirements of the system, the group put together several design alternatives. One involved a tube used to supply the liquid with the patch fastened to the tip. The other design involved a six-well plate with tubes running through the bottom of each well. The group considered the objectives, functions, specifications and constraints as they pertained to

these two designs. A pairwise comparison chart, shown below in Table 4, was used to determine the better design.

	Design	
Objectives	12-well plate	Tube
Prevent water leakage	1	2
Fasten patch	2	1
Multiple tests at a time	2	1
Simulate in vivo forces	2	2
Continuous system	2	2
Measures pressure and change in height	2	2
Totals	11	10

Table 4: Fatigue Apparatus Pairwise Comparison Chart

The results of the pairwise comparison chart indicate that the 12-well plate design is the most effective for this design. This design is not only more efficient, but it also provides a better method of fastening the scaffold. The only way to properly fasten the scaffold to the tube without leakage would be to screw it down; however, since Veritas and UBM is such a delicate material, screwing it down is not a feasible option. The final design is pictured below in Figure 5.

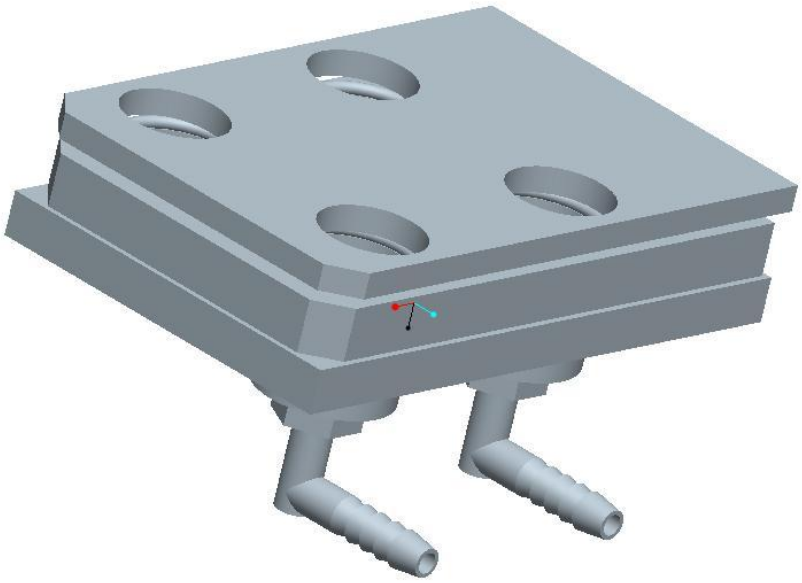

Figure 5: Schematic of Fatigue Apparatus

Using this schematic, the apparatus was built using the following steps. First, the dimensions of a 12-well plate were measured on a sheet of acrylic. Then, using a skill saw, the acrylic was cut into the proper dimensions. The diameter of each well was measured (about one inch each), and four holes of an area given by that diameter were drilled into the acrylic, using a drill press. After that, washers were glued with super glue around each hole and well to seal the cover and the well plate. Following this, holes were drilled in the bottom of the four chosen wells. Teflon tape was placed around the insertion region of the elbow tube connector, and they were inserted into each hole with two washers in between the elbow tube connector and the bottom of the well. Next, tubing was run from each well to the syringes on the syringe pump. The wells were sealed with all-purpose sealant, and the surrounding unused wells were filled with silicone caulking. Finally, washers were attached around each well, and a grommet was fastened around the inner ring of the washers.

5.2 Self-Sealing Test

Once the fatigue test apparatus was built, the group was able to run a self-sealing test on the two biomaterial considerations: UBM and Veritas. A schematic of the test is shown below in Figure 6:

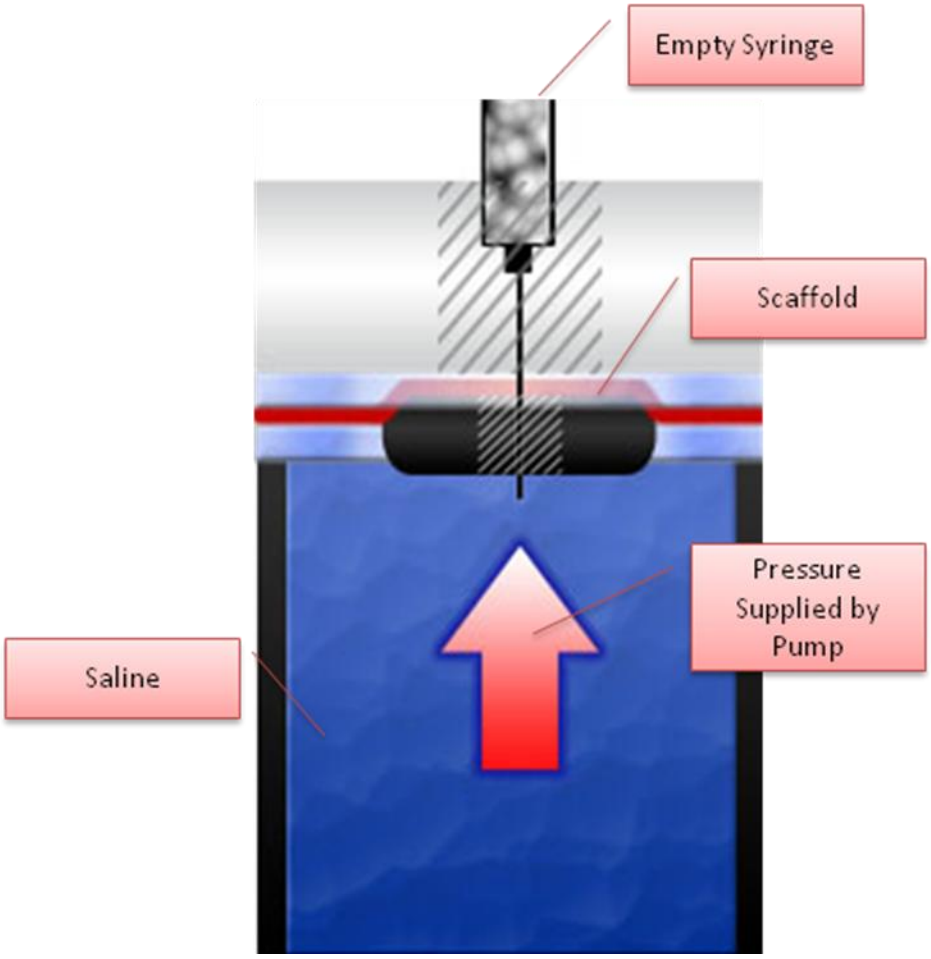

Figure 6: Schematic of Self-Seal Experiment

The materials must have the ability to self-seal in order to prevent leakage from suturing and from puncturing holes during the *in vivo* testing. Since minor leakage of the fatigue apparatus occurred, a control experiment was performed to ensure that leakage does not affect the results. In order to run this test, a given volume of saline was infused into the well of the fatigue apparatus until about 120 mmHg of pressure was applied to the scaffold. In the control experiment the scaffold was not punctured. For the experiment, a syringe needle was used to puncture three holes in the scaffold. If the pressure did not stabilize above 0 mmHg, the scaffold was not considered self-sealing.

5.3 Fatigue Strength Test

Following the self-sealing test was the fatigue strength test. Since UBM was unable to self seal, only Veritas was considered for fatigue strength. Below is a schematic of the test (Figure 7):

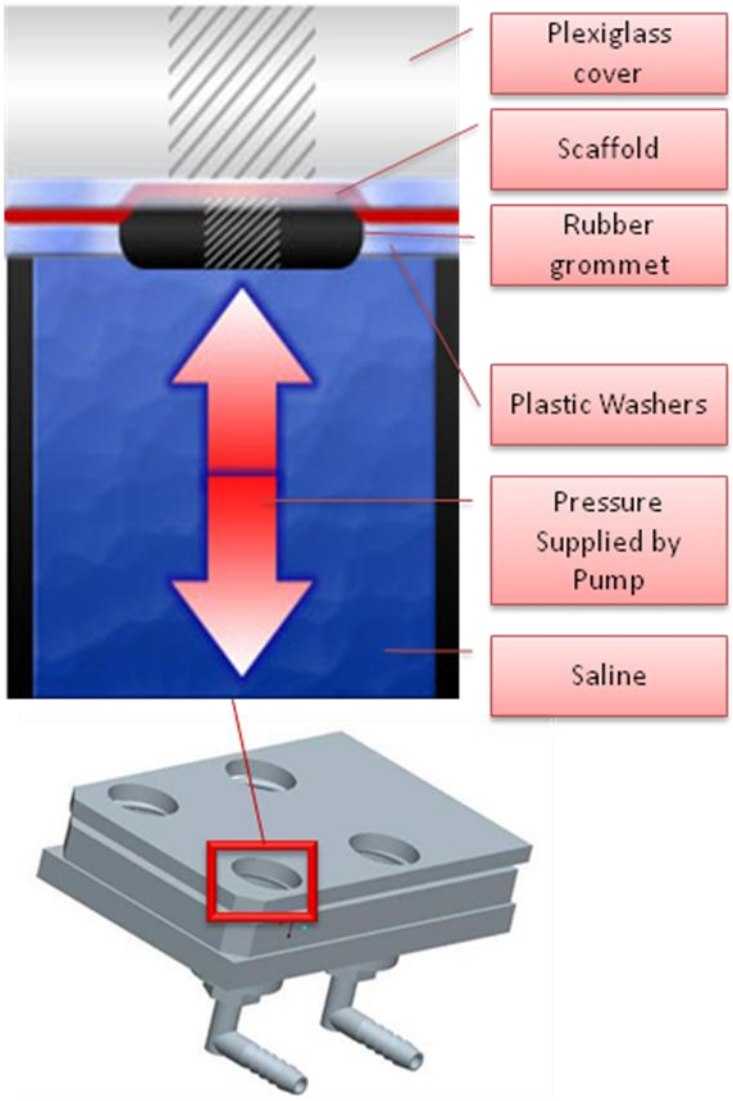

Figure 7: Schematic of Fatigue Strength Experiment

The system (syringe, tubing, and well) was filled with saline. Next, any air in the system was removed. Then, a pressure transducer line was attached through the tubing. This was used to measure the pressure applied to the scaffolds. A sono crystal was sutured to the side of each well. Following this, the Veritas scaffold was placed over the well. Then, a washer was used to fasten the scaffold tightly over the grommet and washer. Finally, using the four clamps, the well cover was tightly held over the well plate so that the four scaffold wells coincided with the holes in the cover. This allowed room for the scaffolds to expand. Then, an additional sono crystal was

sutured over the scaffold. Finally, the apparatus was submerged to a depth of 12.5 mm under water to facilitate signaling between then sono crystals. Plastic wrap was placed over the water vessel in order to create a humidified chamber.

Using LabVIEW 8.0, the syringe pump was programmed to infuse and withdraw the saline at 0.5 Hz for 12 hours, while compensating for any pressure drop by infusing additional volumes of saline. SonoSoft, the program that records the sono crystal output data, was adjusted to the appropriate settings, and measurements of the location of the sono crystals with respect to the apparatus were taken. Crystal placement is indicated in the diagram below (Figure 8).

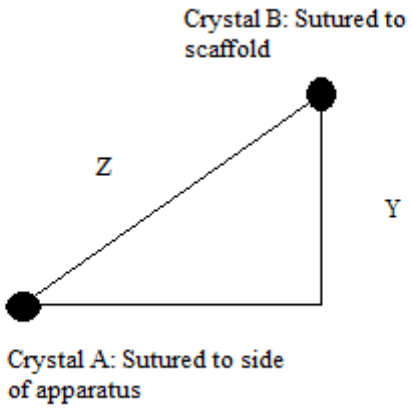

Figure 8: Crystal Placement Diagram

This diagram displays the geometry of the crystals with respect to the apparatus; measurements Z and Y were recorded for each test. Then the data was adjusted for this angular discrepancy in order to obtain the actual change in height of the scaffold. Finally, the results from the transducers were analyzed to ensure that the data reflected a constant expansion height, neglecting any initial changes in the height. In addition, the pressure was checked to ensure that it remained consistent throughout the procedure.

5.4 Cell Loading Test

In order to determine whether or not hMSC's migrate into the Veritas scaffold, quantum dot loaded hMSC's were seeded on Veritas. Veritas scaffolds, with dimensions of 2x2 cm, were placed in a Petri dish. A 16mm diameter O-ring was placed on top of the Veritas and sealed with vacuum grease. The purpose of the O-ring was to hold the media that was concentrated with

20,000 hMSCs. After 7 days, and 14 days, the Veritas was cut into 6 micron cross-sections and histologically analyzed using trichrome staining.

5.5 In Vivo Test

After completing the *in vitro* testing necessary to validate the efficacy of this design for *in vivo* applications, it was essential to implant the scaffold in the rodent model. WPI IACUC approval was obtained in order to purchase nine male Sprague-Dawley, SD, strain (300-350 grams) rodents from Charles River Laboratory. The rodents were housed at the Gateway Park housing facility on the Worcester Polytechnic Institute campus. Due to time constraints, only two surgeries were performed. Both surgeries involved implantation of the scaffold in addition to three punctures with a 30 gauge needle.

Two weeks prior to implantation, a 1x1 cm piece of Veritas was seeded with hMSCs at a cell density of 2×10^5 cells/cm^2. This density lies within the average range of cell seeding on scaffolds as indicated in Table 1. The Veritas was cut and placed in a 12-well plate. Following this, an 8mm diameter washer was placed on top of the Veritas and sealed using vacuum grease. The purpose of the washer was to hold 100 microliters of media, which was concentrated at 100 cells/microliter, on top of the Veritas. The hMSCs were shown to migrate into the Veritas using this method with the previously discussed cell loading assay.

At least three days after the arrival of the rodents, a survival surgery was performed. The rodents were anesthetized using IP Ketamine and Xylazine. The chests were shaved, and the rodents were intubated for ventilation throughout the procedure. Next, a thoracotomy was performed to separate the ribs, using a spring loaded retractor, at the fourth intercostals space. An incision of approximately two centimeters in length was made, and a Veritas patch was sutured over a portion of the left ventricle. The implants were sutured with a 5-0, 6-0, or 7-0 prolene suture. Following implantation, the experiment group received the full thickness punctures with a 30 gauge syringe needle. Once the bleeding subsided, the chests were closed in layers with a combination of 2-0 – 4-0 silk, vicryl and monocryl sutures.

Chapter 6: Results

6.1 Self-Sealing Test

The control experiment, which was performed as outlined in the methodology section, depicted a minor drop in pressure due to leakage in the fatigue apparatus (Figure 9). The self-sealing properties of Veritas and UBM were determined based on the procedures outlined in the methodology section. The UBM was loaded to a pressure of about 120 mmHg on the fatigue apparatus and the scaffold was punctured. Significant leakage occurred immediately after the syringe needle was removed and the pressure dropped to nearly 0 mmHg. A picture of the UBM post-puncture and a graph of the pressure drop are shown below in Figures 10 and 11.

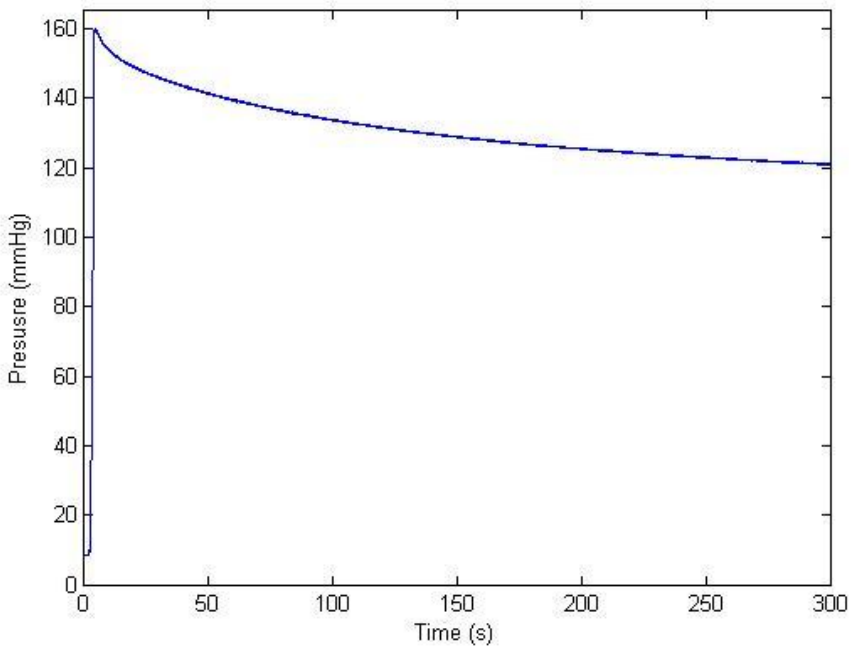

Figure 9: Control Pressure Data

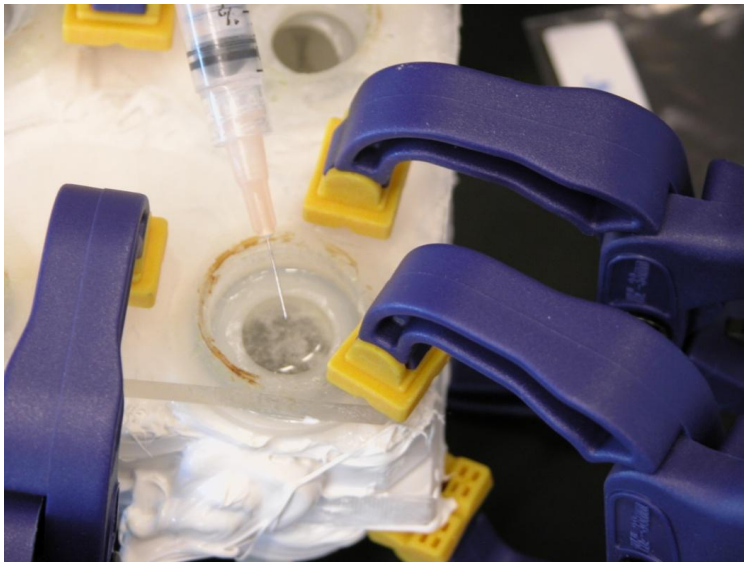

Figure 10: UBM Self-Seal Test

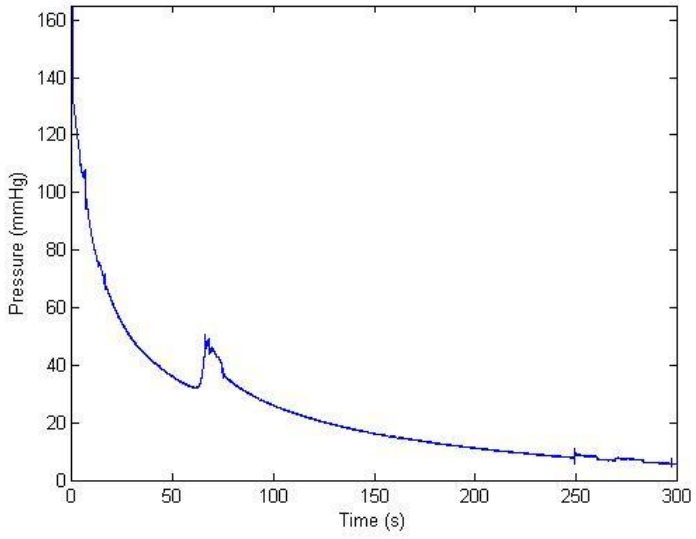

Figure 11: UBM Self-Seal Pressure Data

The picture illustrates the pooling of saline above the UBM scaffold after it was punctured three times. This test determined that UBM does not have self-sealing abilities and therefore is not a viable option.

The Veritas patch was subjected to the same procedure as the UBM patch to determine if it possessed the essential self-sealing property that is required for the scaffold design. After the Veritas patch was punctured by the syringe needle, the pressure dropped gradually and eventually equilibrated after 300 seconds at 50 mmHg (Figure 12). After this time period, the pressure held constant and the leakage ceased. The results of this test determined that the Vertias

scaffold showed a self-sealing capability; therefore, additional tests were conducted to determine if this material had the necessary characteristics to be incorporated into the design.

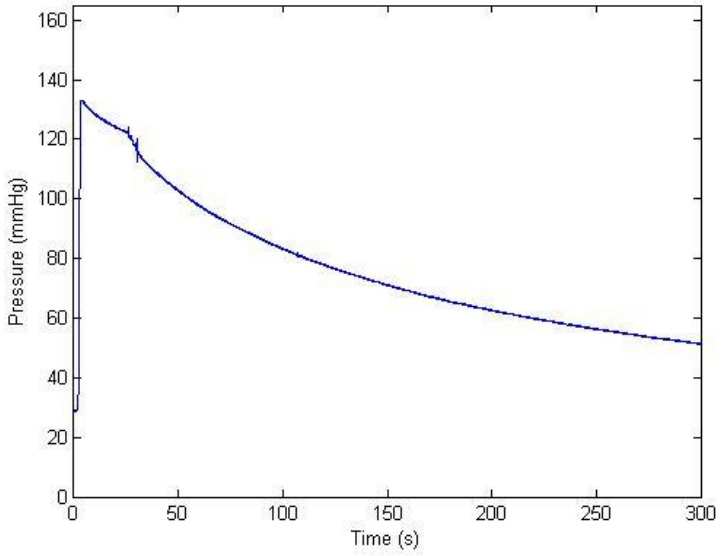

Figure 12: Veritas Self-Seal Pressure Data

6.2 Fatigue Strength Test

The fatigue strength test was more complicated than initially anticipated. There were several factors that dramatically changed the initial design of the fatigue apparatus. The first issue was the persistent leakage at various locations. The next factor was the large deformation that the Veritas underwent during the cyclic loading. After 24 hours, the deformation that the Veritas scaffold underwent caused a significant drop in pressure. This drop in pressure meant that the Veritas scaffold was no longer being loaded to a maximum of 120 mmHg. The drop in pressure can be seen in the Figures 13-15 below.

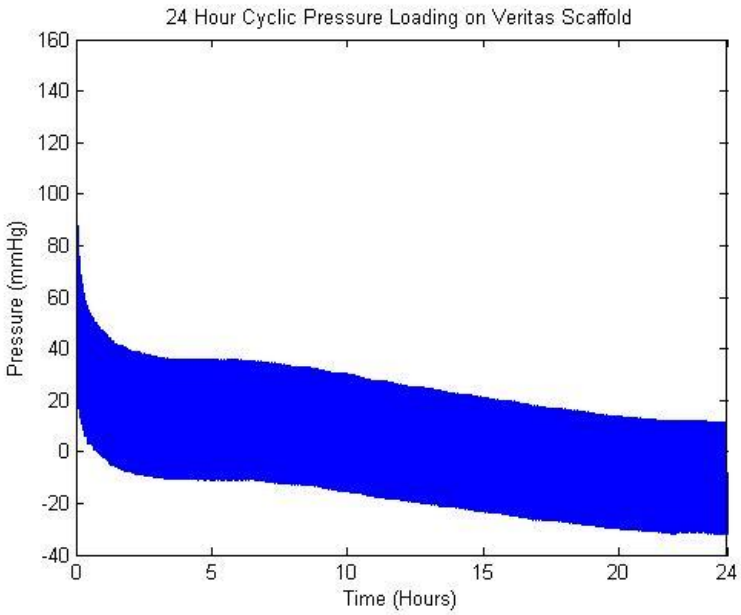

Figure 13: 24 Hour Cyclic Pressure Loading on Veritas Scaffold

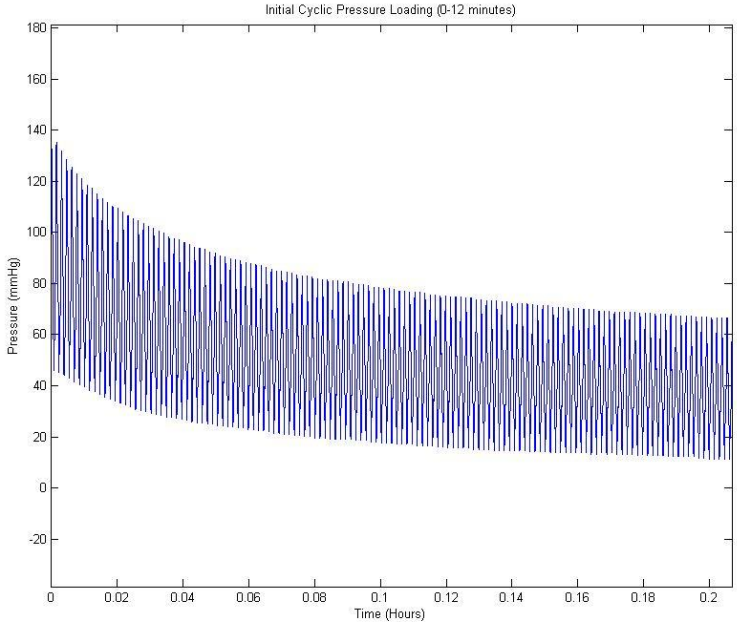

Figure 14: Initial Cyclic Pressure Loading (0-12 minutes)

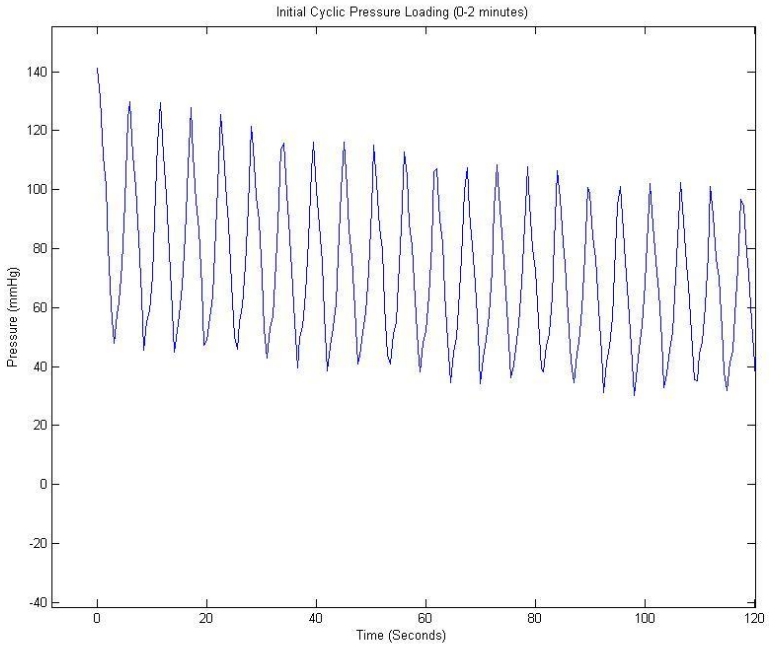

Figure 15: Initial Cyclic Pressure Loading (0-2 minutes)

Since the fatigue strength test was designed to replicate the forces that the Veritas scaffold experiences post-implantation, the pressure on the patch must cycle from 5 mm Hg to 120 mmHg consistently for the duration of the experiment. The first problem was resolved by several modifications to the initial design that reduced the leaking to a minimum. The second problem required the use of LabVIEW 8.0, which was used to control the syringe pump, as previously described, to increase the saline infusion volume when the pressure dropped below 120 mmHg. This program maintained the necessary pressures that were required for the results of the experiment to be considered valid.

The fatigue test results show that the Veritas deforms slowly initially and undergoes minor deformation during the final hours of the experiment. As shown in Figure 16, the initial displacement of the Veritas was approximately 1.72 mm. After about 12 minutes, the displacement increased to roughly 4.25 mm and remained consistent for nearly three hours. As shown in Figure 17, the pressure stayed relatively consistent for the initial 30 minutes. Figures 18 and 19 are zoomed in displacement and pressure graphs that show the details of the waveforms. After 3.6 hours, a minor increase in displacement of 0.25 mm occurred (Figure 20). The pressure data for this time period was also consistently at 130 mmHg (Figure 21). At 8 hours, another increase in displacement of 1.5 mm was observed (Figure 22). This time period's

pressure data increased slightly to 135 mmHg (Figure 23). After 11 hours, the displacement actually decreased by 0.4 mm (Figure 24). The pressure data remained the same at 11 hours (Figure 25).

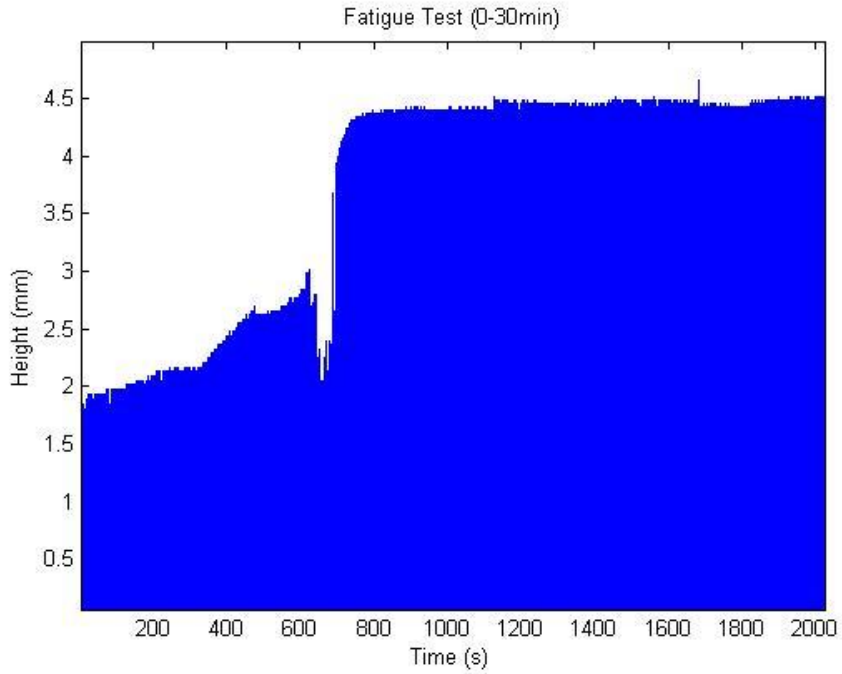

Figure 16: Fatigue Test Displacement Data (0-30 min)

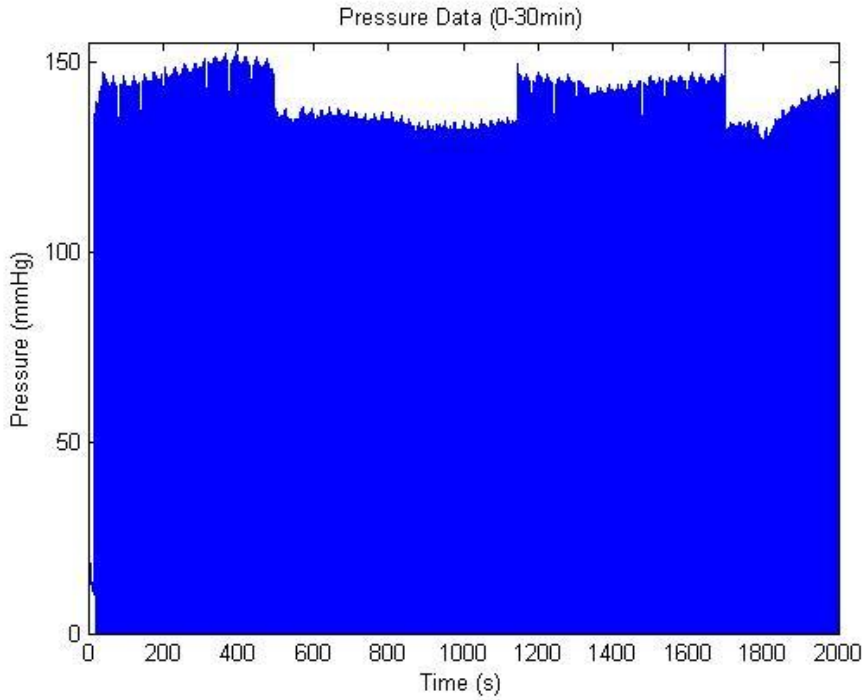

Figure 17: Fatigue Test Pressure Data (0-30 min)

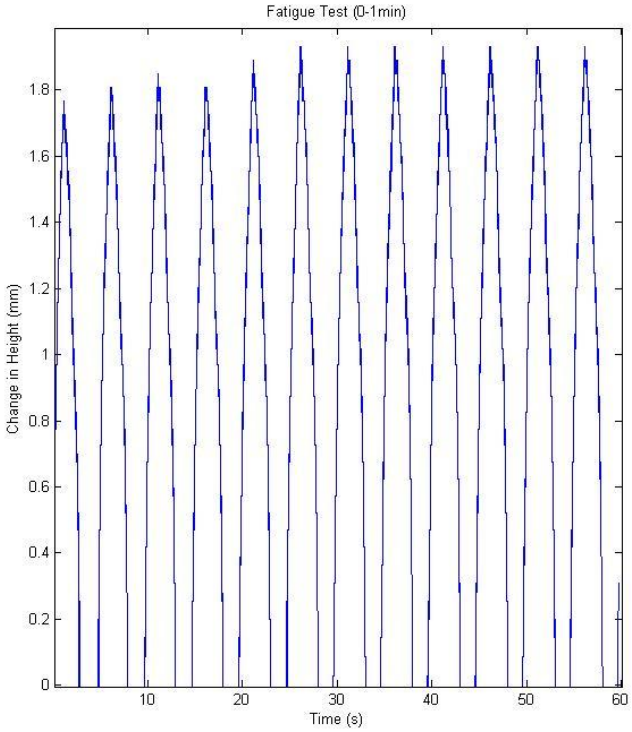

Figure 18: Fatigue Test Displacement Data (0-1 min)

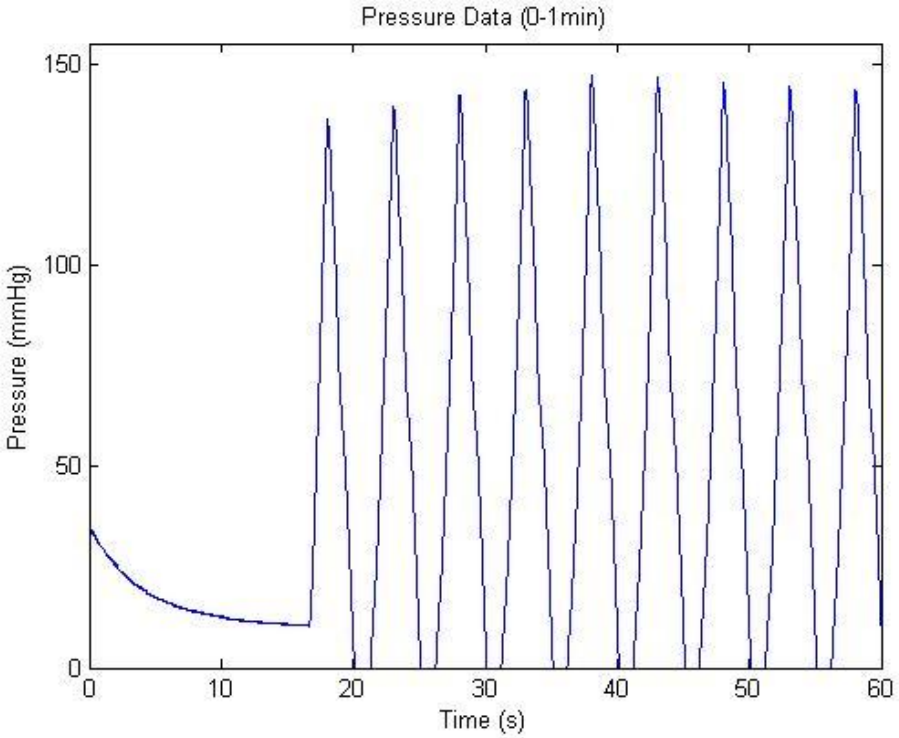

Figure 19: Fatigue Test Pressure Data (0-1 min)

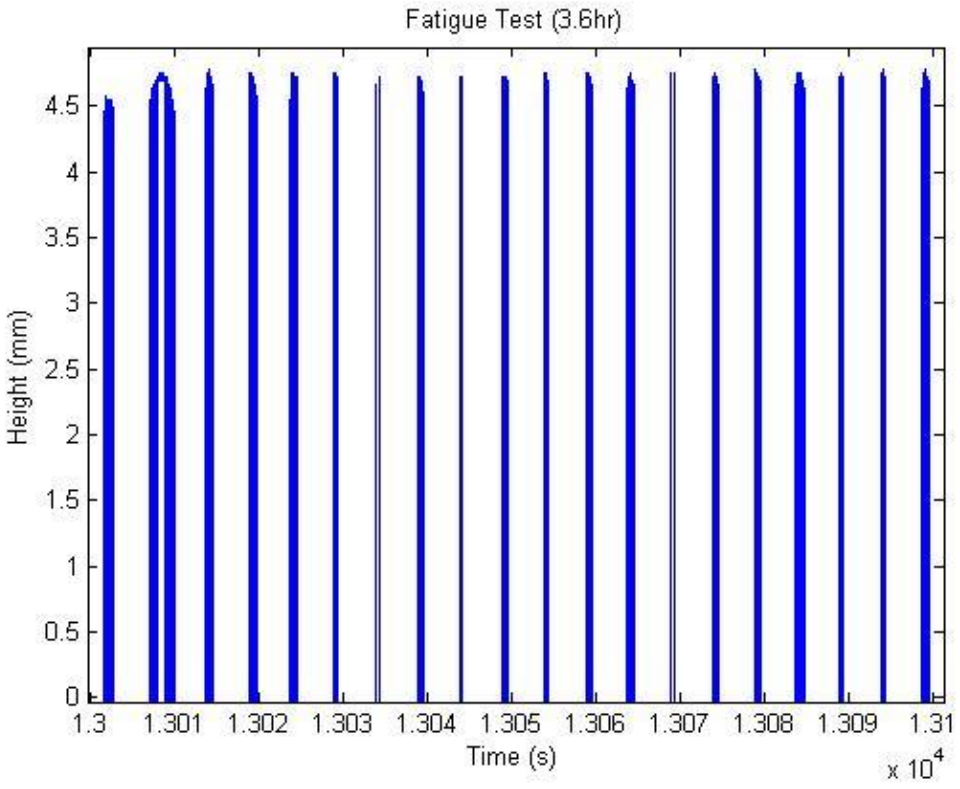

Figure 20: Fatigue Test Displacement Data (3.6 hr)

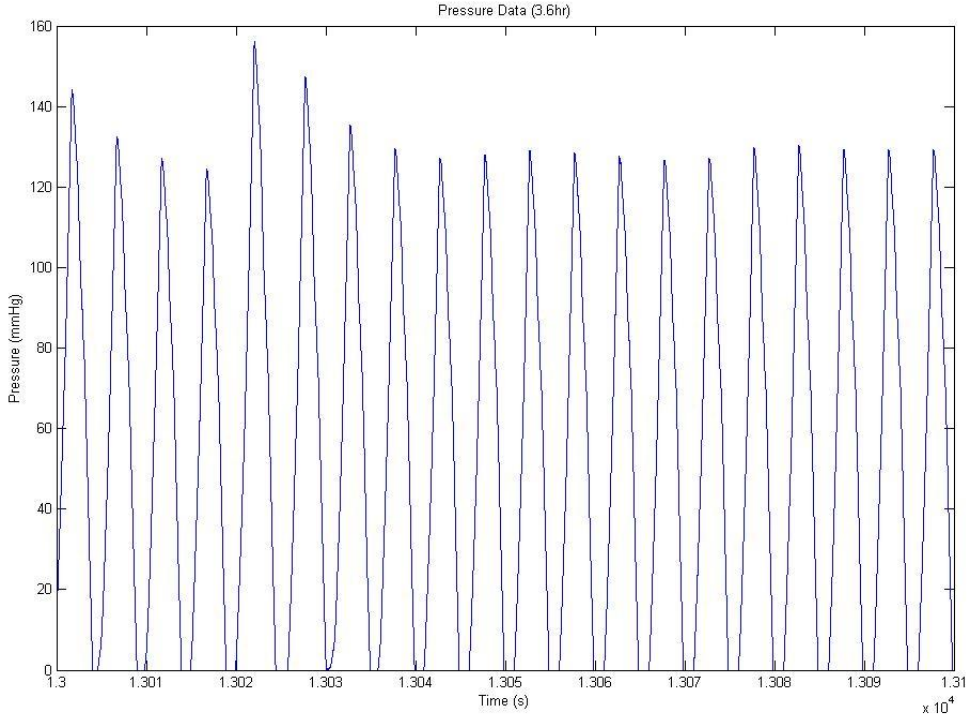

Figure 21: Fatigue Test Pressure Data (3.6 hr)

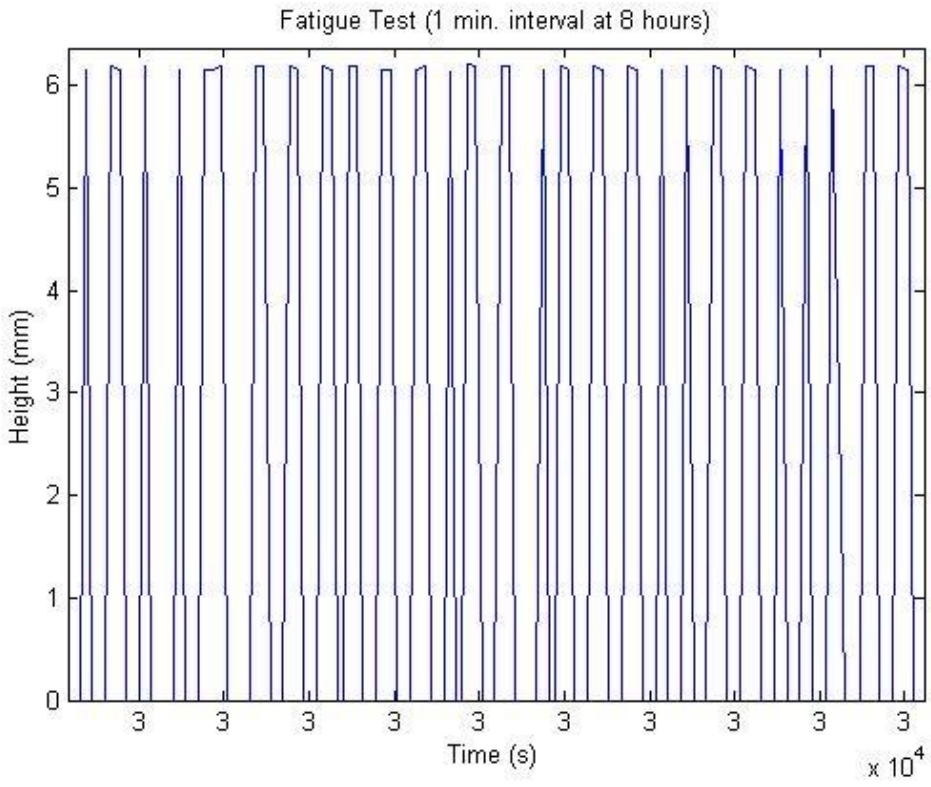

Figure 22: Fatigue Test Displacement Data (8 hrs)

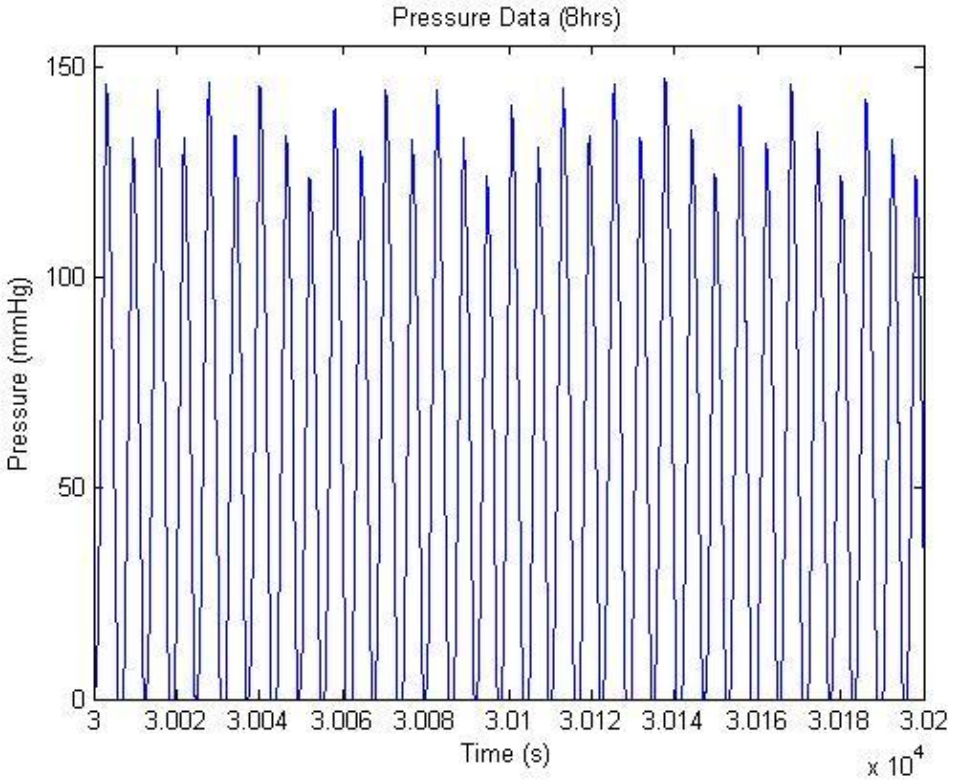

Figure 23: Fatigue Test Pressure Data (8 hrs)

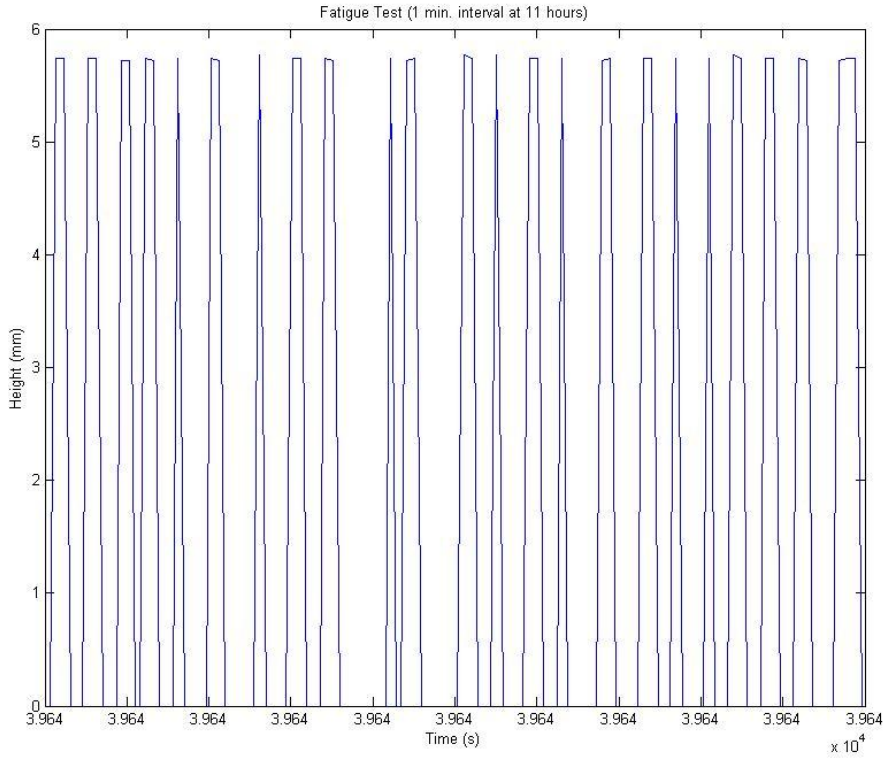

Figure 24: Fatigue Test Displacement Data (11 hrs)

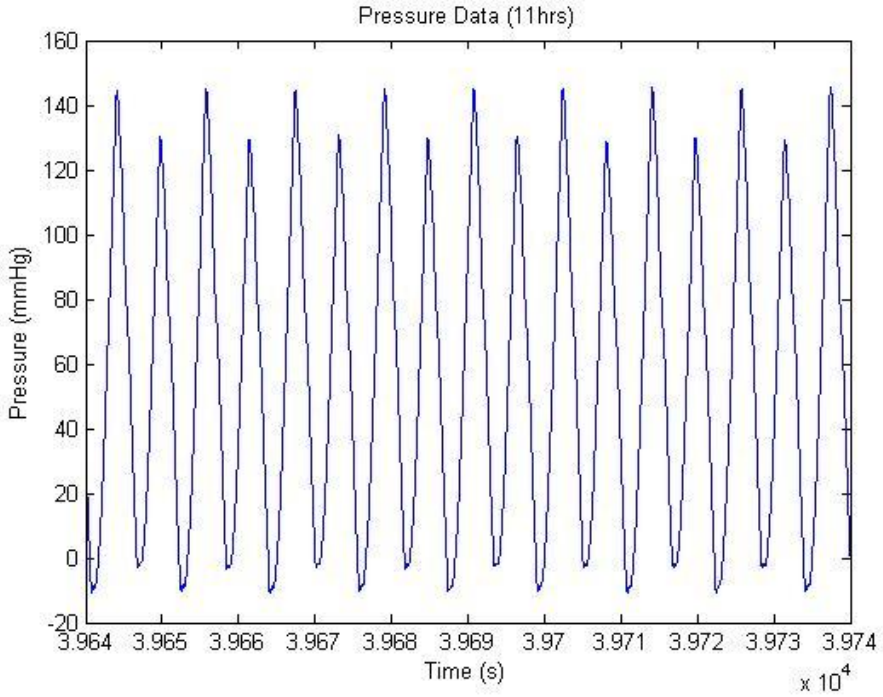

Figure 25: Fatigue Test Pressure Data (11 hrs)

6.3 Cell Loading Test

The cell loading test was essential for determining the time period that was required to allow the hMSCs to migrate into the Veritas scaffold prior to implantation. About 20,000 hMSC's were seeded on a 2cm x 2cm section of Veritas. Figure 26 is a control trichrome stain of unseeded Veritas.

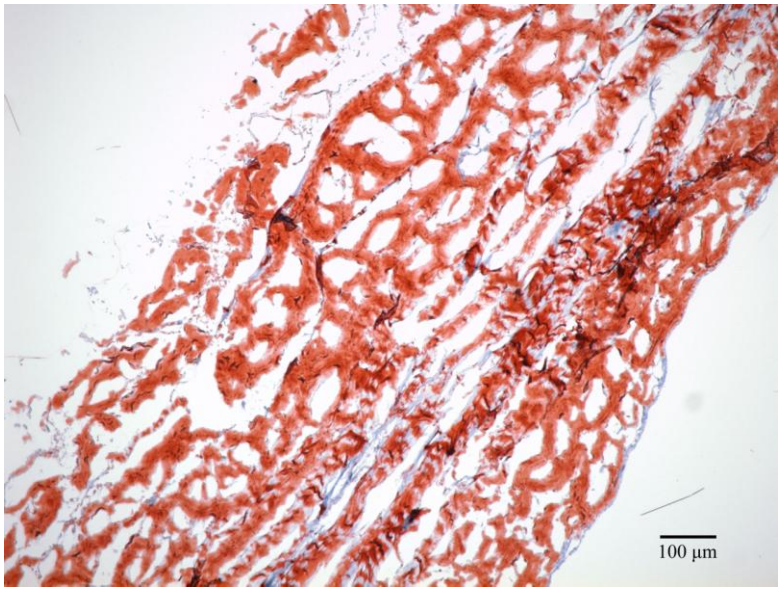

Figure 26: Trichrome Control of Unseeded Veritas

After 24 hours, no cell migration occurred. Figure 27 is an image of a trichrome stain on Veritas that was seeded for 7 days. The cell furthest from the top seeded portion of the Veritas migrated 800 µm into the scaffold.

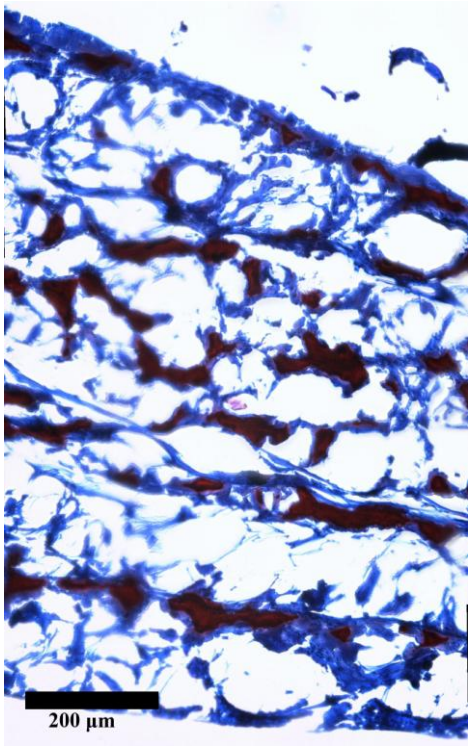

Figure 27: Trichrome Seeded for 7 Days

Figure 28 is an image of a trichrome stain on Veritas that was seeded for 14 days. The cell furthest from the top seeded portion of the Veritas migrated 1200 µm.

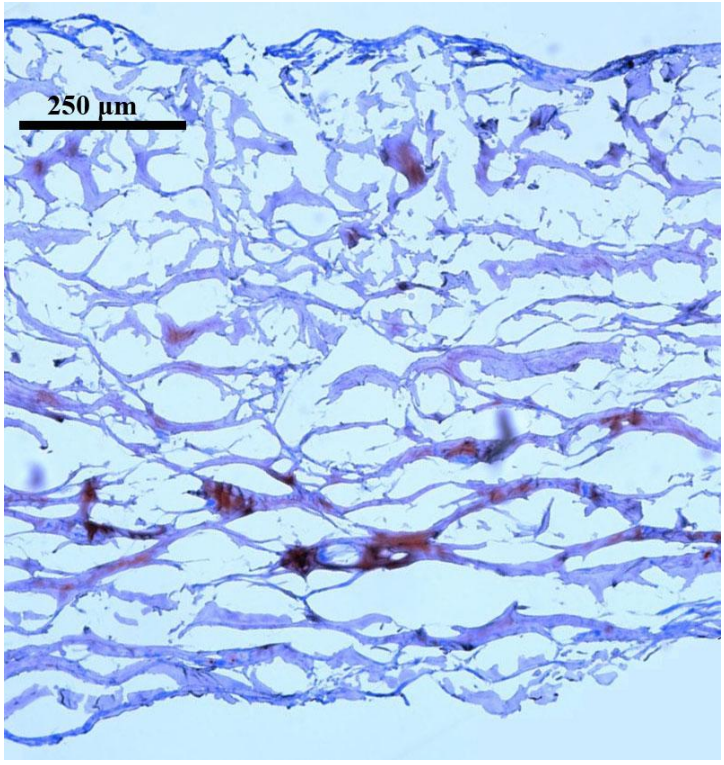

Figure 28: Trichrome Seeded for 14 Days

The purpose of this experiment was to find the ideal duration of seeding time prior to implantation, which would enable larger densities of hMSCs to be seeded onto the scaffold. Below is a graph (Figure 29) that analyzes migration distance over time. From this graph it can be determined that the optimal seeding time is from 10 to 16 days.

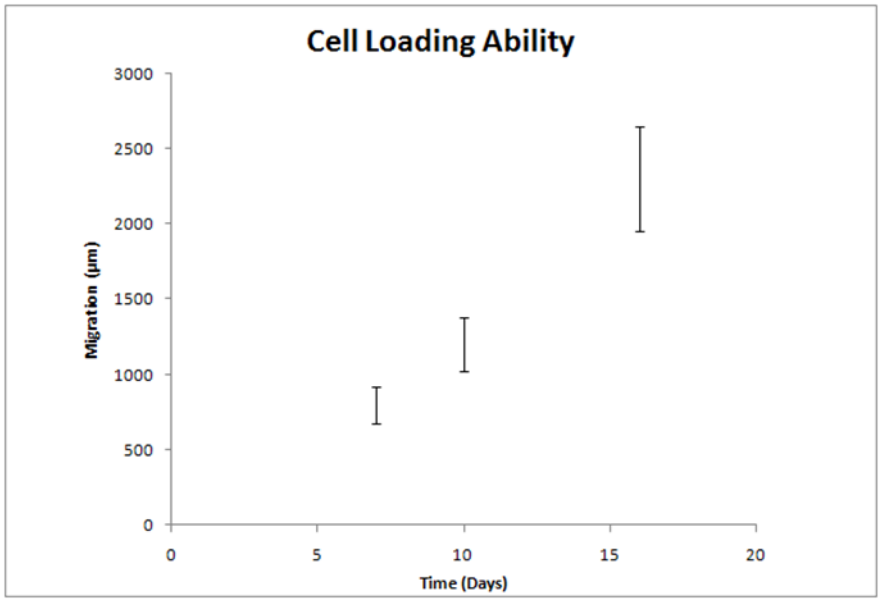

Figure 29: Results of Cell Loading Test

6.4 In Vivo Results

Two groups, each consisting of eight scaffolds, were seeded about three weeks prior to implantation. From each group, four scaffolds were taken for histological analysis. Two scaffolds were taken at 10 days, and two were taken at 16 days. Each was histologically analyzed using trichrome staining. Figure 30 is an image of the group 1 Veritas after 10 days. Figure 31 is an image of the group 1 Veritas after 16 days.

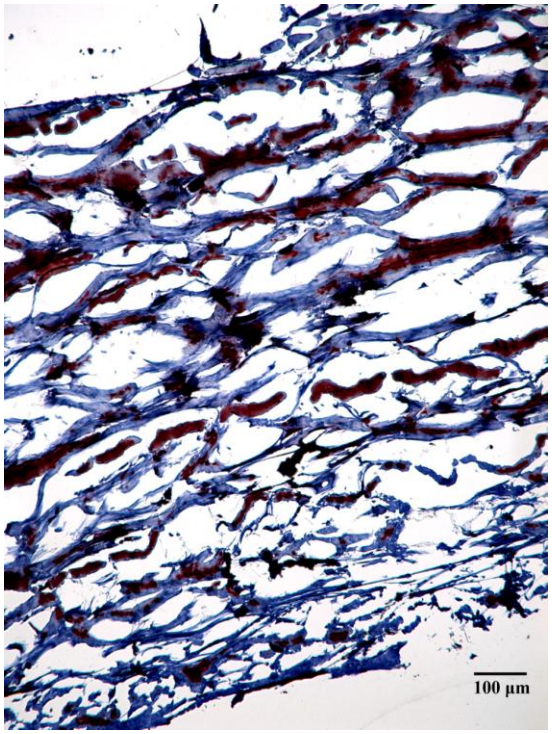

Figure 30: Group 1 Veritas at 10 Days

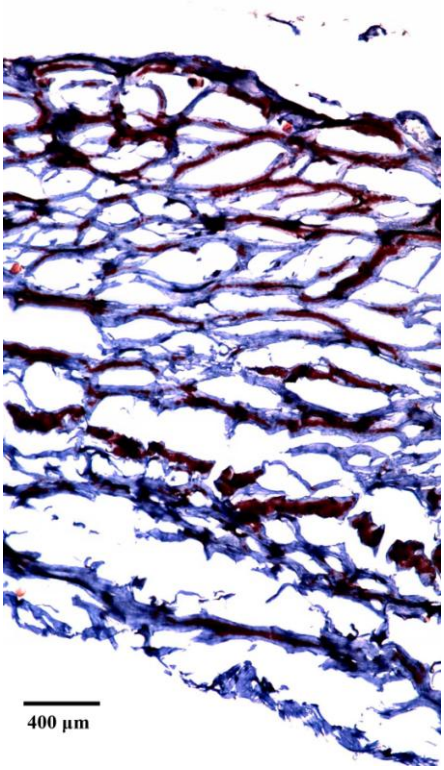

Figure 31: Group 1 Veritas at 16 Days

The furthest cell in the 10 day group 1 image migrated about 1200μm. The furthest cell in the 16 day group 1 image migrated about 2800 μm. The analysis of these scaffolds was used to ensure that the implanted scaffolds were optimally seeded.

After about three weeks of scaffold culturing time, two scaffolds were implanted in rodents. Due to time constraints, only two surgeries were performed; however, both were successful in implanting the design. The first rodent weighed about 300g. About 30 minutes before the procedure, it was administered 0.7mL Ketamine and 0.1mL Xylazine. Minutes prior to the implantation of the scaffold, the rodent died due to a technical error in the ventilation system. The scaffold was still successfully implanted since the rodent died from errors unrelated to the design. The second rodent weighed about 350g. Thirty minutes prior to surgery, the rodent was administered 0.85mL Ketamine and 0.1mL Xylazine. During the procedure, the rodent died due to small incision in the lung. This procedure resulted in successful implantation of the scaffold, and the death of the rodent was unrelated to the design.

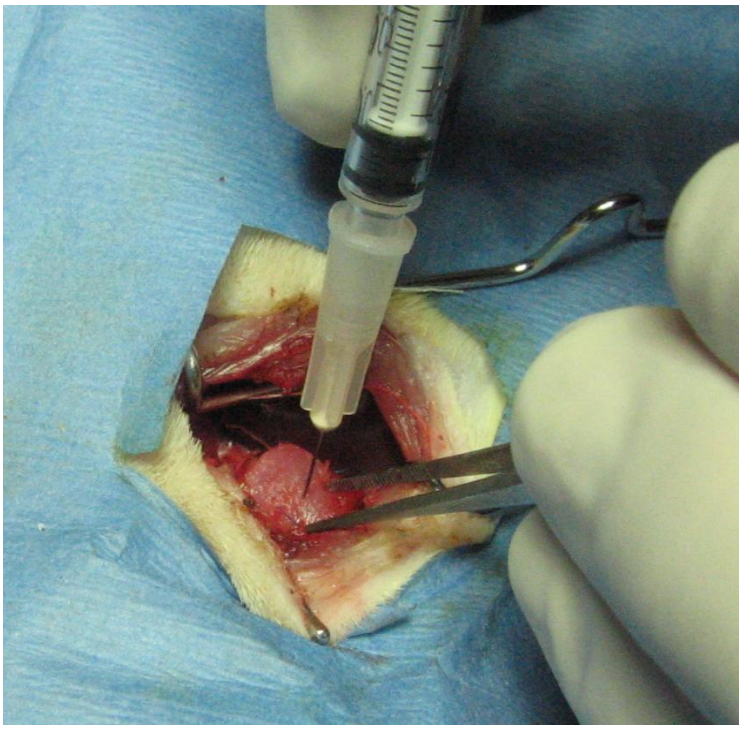

Figure 32: Application of the Final Design in the Rodent Heart

Figure 32 shows the successful application of the design in the rodent heart during the procedure. As a result of two successful implantations of the design, it was determined that this design is surgically simple and clinically applicable.

Chapter 7: Analysis and Discussion

The purpose of much of the *in vitro* testing was not only to qualify the efficacy of the design, but also to determine the benefits of certain design components. The first test, the self-sealing test, was used not only to determine the efficacy of the two biomaterials, but also to determine the better scaffold choice for this design. The results of the self-seal test indicated that UBM did not have the ability to self-seal; however, Veritas did have this ability. Therefore, the test not only removed UBM from the biomaterial scaffold considerations, but it also advanced Veritas onto further testing.

As shown in Figure 10, the graph of the UBM pressure decreases post-needle puncture. This detail along with the pooling of saline above the scaffold in the apparatus indicated that UBM did not have self-sealing potential. One note that must be addressed about this graph is the slight peak about half way through the decrease in pressure. This was a result of an accidental disturbance of the apparatus during the pressure recording time. Since human error was a result of this discrepancy, it can be disregarded.

The self-seal test for Veritas was more successful than that of the UBM. The pressure was shown to stabilize after 300 seconds at 60 mmHg. While this data proves that Veritas self-seals, it was expected that the Veritas would self-seal at a faster rate; however, the leaky apparatus may have attributed to the decrease in pressure. Nonetheless, Veritas displayed the necessary self sealing ability as stated by the specifications.

Following the self-seal test, Veritas was tested for its fatigue strength, which was an additional design criterion previously specified. The initial testing of Veritas resulted in failure; however, these results were mostly due to a failure in the apparatus. Leakage occurred over the course of the 24 hour period, resulting in a decrease in the infusion volume, which therefore decreased the pressure applied on the scaffold. Figures 11-13 illustrate this response. One note on the graphs is needed to explain the rough cycle waveform. This was not only due to down-sampling of the data, which was done in order to graph the information, but it was also due to a skip that occurred consistently in the cycles due to the syringe pump.

Due to consistent pressure drops during the fatigue testing, LabVIEW programming was required to apply a consistent pressure thereby varying the infusion volume. As a result, the data

in Figures 16-25 was acquired. More deformation occurred than was expected; however, overall (not including the initial deformation) the displacement only increased by about 2 mm throughout the 12 hour period. The pressure data did not vary by more than 10 mmHg. The variation was due to the delay between the acquisition of the pressure data and the reaction of the LabVIEW program. Further testing is necessary for more conclusive data on the fatigue strength of Veritas.

The results of the migration test were crucial in determining the cell-seeding time prior to implantation. The migration tests not only ensured that hMSCs have the ability to migrate through the scaffold, implying that they can also migrate out, but the test also showed that increased cell densities can be seeded on the scaffold. If an increase in cell density was desired, then initial cell seedings could allow cells to migrate into the scaffold for a given amount of time followed by subsequent surface seedings. This would improve chances of myocardial regeneration by increased cell saturation, cell viability, increased proliferative potential of cardiac myocytes, and/or increased differentiation of the stem cells. In addition, the histology figures of the cell loading assay were acquired while the method of cell seeding on the Veritas was still being perfected. As a result, it can be assumed that subsequent seedings of hMSCs on Veritas will result in an increase in the abundance of cells and potentially further cell migration.

Finally, the results of the in vivo testing proved the surgical simplicity and clinical applicability of the design. Due to technical errors, both rodents perished during the surgery; however, a novice surgeon was still able to implant the scaffold. Therefore, since the deaths were unrelated to the implantation method, it was concluded that the design was successfully implanted.

Chapter 8: Conclusions

Based on *in vitro* and *in vivo* tests that were completed, it can be concluded that this design is a clinically applicable device for use in the surgical treatment of ventricular aneurysms. As mentioned, Filipe et al.[8] proved that both UBM and Veritas scaffold materials contain the necessary mechanical properties for cardiac applications. These include tensile strength, strain, and suturability. The design presented in this project concludes that Veritas meets all additional specifications as defined by the parameters to be a used as a clinically applicable scaffold for cardiac regeneration.

The UBM scaffold material was unable to self seal after five minutes following three syringe punctures. Due to this failed test it was concluded that UBM would not be an appropriate scaffold material for this application. The Veritas did sufficiently seal following the five minute self-seal test. From these results, it was concluded that Veritas would be the chosen material for the final design.

The next test completed was the fatigue test. The Veritas fatigue test was run three independent times. Results from this test indicate that Veritas reached a maximum deformation of approximately 5.7mm. This was acceptable for the given specifications. These results indicate that Veritas will be able to withstand the forces of the heart over a long term period, ensuring that the design presented in this project is clinically applicable.

The cell loading test was done to ensure that the cells could be successfully loaded onto the scaffold material. Following the seeding of the cells and the 16 day intubation period, it was found that the cells migrated a maximum distance of 2800μm into the scaffold material. It can be concluded that Veritas provides a sufficient cell loading ability. This ability can lead to a proper delivery method of cells into the heart following infarction.

The final test of the efficacy of the design was the *in vivo* implantation. The scaffolds were implanted onto the ventricular wall of male Sprague-Dawley rats and the scaffold material was punctured. The scaffolds were successfully implanted by a novice surgeon. Based on the results of this test, it was concluded that the design facilitates surgical simplicity.

Following all *in vitro* and *in vivo* tests it can be concluded that the design is a novel method of safely delivering hMSCs to the heart. Based on the functions, specifications,

constraints, and objectives the design has accomplished what was desired. It has the necessary mechanical properties to be effective as well as the porosity needed to self seal and load cells.

Overall, it can be concluded that the problem given in the initial client statement was solved. A clinically applicable scaffold, which may aid in cardiac regeneration, was successfully designed and implanted. However, further *in vivo* testing must be done to determine if the final design induces cardiac regeneration.

Chapter 9: Future Recommendations

There are many aspects of this project that were not pursued due to time and financial constraints. The $468 budget and the eight month deadline were limiting factors in the amount of research that could be completed. This section details suggestions for future research.

The fatigue apparatus was vital for characterization of a scaffold for use in cardiac regeneration. Many problems were encountered during the manufacturing process that diminished the accuracy of the obtained data. Future implementations of the fatigue apparatus should include a non-modular construction, a higher quality syringe pump, a unified data collection system, and a less intricate tubing system. Significant leakage occurred during experimentation due to the modular construction of the apparatus and the complex tubing system. Mechanical complications with the syringe pump caused minute discrepancies in the pressure and height waveforms. The use of two computer systems for data collection during the fatigue test increased the probability of inaccuracy, increased the size of the fatigue apparatus package, and required complex manipulation of the data for analysis. Execution of these recommendations may provide more accurate results.

The chosen design uses saline filled syringes that are injected through the scaffold and the ventricular wall. The saline solution can be augmented with possible additives that may assist in new tissue growth. These additives were omitted due to budget constraints. The first additive that could be considered is vascular endothelial growth factor (VEGF). VEGF is a naturally occurring growth factor that induces angiogenesis and increases endothelial permeability[45]. Studies have shown that VEGF enhances endothelialization, which is vital for cell survival and proliferation.[43] Matrix metallo-proteinases (MMPs) are an additional additive that could be incorporated into the design. MMPs are enzymes that control ECM remodeling following infarction.[44] The use of MMPs may encourage new tissue formation through the degradation of scar tissue. Therefore it is recommended that using paracrine factors may improve new tissue formation over stem cells alone.

The surgery that was performed for this project required more time and funding that was allotted. As a result, future studies should incorporate a larger sample size and a longer implantation period. Due to budget constraints, only eight rats were purchased. Increasing the

sample size will allow a more accurate statistical analysis. Due to time constraints, there was no implantation period. Extending the implantation period may provide more developed results.

The ultimate goal of this research is to provide an implantable scaffold that assists in the treatment of ventricular aneurysms and myocardial infarction. The financial and time constraints limited the incorporation of the components presented in this section. The recommendations presented here may lead to more constructive findings.

Bibliography

1. Miniño A, Heron M, Murphy S, Kochanek K. Deaths: final data for 2004. *Natl Vital Stat Rep.* 2007;55(19):1-119.

2. Marieb EN, Hoehn K. *Human Anatomy and Physiology*. 7 ed: Pearson; 2007.

3. Thom T, Haase N, Rosamond W, Howard V, Rumsfeld J, Manolio T, Zheng Z, Flegal K, O'Donnell C, Kittner S, Lloyd-Jones D, Goff DJ, Hong Y, Adams R, Friday G, Furie K, Gorelick P, Kissela B, Marler J, Meigs J, Roger V, Sidney S, Sorlie P, Steinberger J, Wasserthiel-Smoller S, Wilson M, Wolf P. Heart disease and stroke statistics--2006 update: a report from the American Heart Association Statistics Committee and Stroke Statistics Subcommittee. *Circulation.* 2006;113(6):e85-151.

4. Rackley C. Elderly patients at risk for coronary heart disease or stroke: selecting an ideal product for lipid lowering. *Am J Geriatr Cardiol.* 2001;10(2):77-82; quiz 82-74.

5. Hoffman MS. The World Almanac and Book of Facts. Newspaper Enterprise Association; 1995.

6. Cicala R. *The Heart Disease Sourcebook*: RGA Publishing Group; 1997.

7. Association AH. Heart and Stroke Facts. 2003.

8. Filipe DV, McBride NS, Murphy MK, Singh DA. *Design of a Composite Scaffold for Myocardial Regeneration Following Infarction*: Worcester Polytechnic Institute; 2007.

9. Humphrey JD. *Cardiovascular solid mechanics : cells, tissues, and organs*. New York: Springer; 2002.

10. Sherwood L. *Human physiology : from cells to systems*. 4th ed. Pacific Grove, Calif.: Brooks/Cole; 2001.

11. Britannica E. human cardiovascular system. 2007.

12. Cramer DV, Podesta LG, Makowka L. *Handbook of Animal Models in Transplantation Research*: CRC Press, Inc.; 1994.

13. Lee T, Lin M, Chang N. Effect of Pravastatin on Sympathetic Reinnervation in Post-infarcted Rats. *Am J Physiol Heart Circ Physiol.* 2007.

14. Wiley InterScience (Online service). Wiley encyclopedia of biomedical engineering. Hoboken, N.J.: Wiley-InterScience; 2006.

15. Illustrated Stedman's Medical Dictionary. 24th ed. Baltimore: Williams & Wilkins; 1982.

16. Sutton M, Sharpe N. Left ventricular remodeling after myocardial infarction: pathophysiology and therapy. *Circulation.* 2000;101(25):2981-2988.

17. Ford LE. *Muscle physiology and cardiac function*. Traverse City, MI: Biological Sciences Press/Cooper Pub. Group; 2000.

18. Christman K, Lee R. Biomaterials for the treatment of myocardial infarction. *J Am Coll Cardiol.* 2006;48(5):907-913.

19. Dor V, Sabatier M, DiDonato M, Montiglio F, Toso A, Maioli M. Efficacy of endoventricular patch plasty in large postinfarction akinetic scar and severe left ventricular dysfunction: comparison with a series of large dyskinetic scars. *The Journal of Thoracic and Cardiovascular Disease.* 1998;116:50-59.

20. Doss M, Martens S, Sayour S, Hemmer W. Long term follow up of left ventricular function after repair of left ventricular aneurysm. A comparison of linear closure versus patch plasty. *Eur J Cardiothorac Surg.* 2001;20(4):783-785.

21. Eiberg J, Røder O, Stahl-Madsen M, Eldrup N, Qvarfordt P, Laursen A, Greve M, Flörenes T, Nielsen O, Seidelin C, Vestergaard-Andersen T, Schroeder T. Fluoropolymer-coated dacron versus PTFE grafts for femorofemoral crossover bypass: randomised trial. *Eur J Vasc Endovasc Surg.* 2006;32(4):431-438.

22. Murry C, Soonpaa M, Reinecke H, Nakajima H, Nakajima H, Rubart M, Pasumarthi K, Virag J, Bartelmez S, Poppa V, Bradford G, Dowell J, Williams D, Field L. Haematopoietic stem cells do not transdifferentiate into cardiac myocytes in myocardial infarcts. *Nature.* 2004;428(6983):664-668.

23. Müller P, Pfeiffer P, Koglin J, Schäfers H, Seeland U, Janzen I, Urbschat S, Böhm M. Cardiomyocytes of noncardiac origin in myocardial biopsies of human transplanted hearts. *Circulation.* 2002;106(1):31-35.

24. Anversa P, Kajstura J. Ventricular myocytes are not terminally differentiated in the adult mammalian heart. *Circ Res.* 1998;83(1):1-14.

25. Hirzel H, Nelson G, Sonnenblick E, Kirk E. Redistribution of collateral blood flow from necrotic to surviving myocardium following coronary occlusion in the dog. *Circ Res.* 1976;39(2):214-222.

26. Vacanti J, Langer R. Tissue engineering: the design and fabrication of living replacement devices for surgical reconstruction and transplantation. *Lancet.* 1999;354 Suppl 1:SI32-34.

27. Park H, Radisic M, Lim J, Chang B, Vunjak-Novakovic G. A novel composite scaffold for cardiac tissue engineering. *In Vitro Cell Dev Biol Anim.* 2005;41(7):188-196.

28. Archie JJ. A fifteen-year experience with carotid endarterectomy after a formal operative protocol requiring highly frequent patch angioplasty. *J Vasc Surg.* 2000;31(4):724-735.

29. Karas T, Gregoric I, Frazier O, Reul R. Delayed left ventricular pseudoaneurysms after left ventricular aneurysm repairs with the CorRestore patch. *Ann Thorac Surg.* 2007;84(1):266-269.

30. Zippel R, Wilhelm L, Marusch F, Koch A, Urban G, Schlosser M. Antigenicity of polyester (Dacron) vascular prostheses in an animal model. *Eur J Vasc Endovasc Surg.* 2001;21(3):202-207.

31. Connolly R. Evaluation of a unique bovine collagen matrix for soft tissue repair and reinforcement. *Int Urogynecol J Pelvic Floor Dysfunct.* 2006;17 Suppl 1:S44-47.

32. Robinson K, Li J, Mathison M, Redkar A, Cui J, Chronos N, Matheny R, Badylak S. Extracellular matrix scaffold for cardiac repair. *Circulation.* 2005;112(9 Suppl):I135-143.

33. Gibble J, Ness P. Fibrin glue: the perfect operative sealant? *Transfusion.* 1990;30(8):741-747.

34. Christman K, Vardanian A, Fang Q, Sievers R, Fok H, Lee R. Injectable fibrin scaffold improves cell transplant survival, reduces infarct expansion, and induces neovasculature formation in ischemic myocardium. *J Am Coll Cardiol.* 2004;44(3):654-660.

35. Dimmeler S, Zeiher A, Schneider M. Unchain my heart: the scientific foundations of cardiac repair. *J Clin Invest.* 2005;115(3):572-583.

36. Orlic D, Kajstura J, Chimenti S, Jakoniuk I, Anderson S, Li B, Pickel J, McKay R, Nadal-Ginard B, Bodine D, Leri A, Anversa P. Bone marrow cells regenerate infarcted myocardium. *Nature.* 2001;410(6829):701-705.

37. Potapova IA DS, Kelly DJ, Rosen AB, Schuldt AJ, Lu Z, et al. Regeneration of the Canine Ventricle Using Adult Human Mesenchymal Stem Cells. *Circ Res.* 2006.

38. Min J, Sullivan M, Yang Y, Zhang J, Converso K, Morgan J, Xiao Y. Significant improvement of heart function by cotransplantation of human mesenchymal stem cells and fetal cardiomyocytes in postinfarcted pigs. *Ann Thorac Surg.* 2002;74(5):1568-1575.

39. Conconi M, De Coppi P, Bellini S, Zara G, Sabatti M, Marzaro M, Zanon G, Gamba P, Parnigotto P, Nussdorfer G. Homologous muscle acellular matrix seeded with autologous myoblasts as a tissue-engineering approach to abdominal wall-defect repair. *Biomaterials.* 2005;26(15):2567-2574.

40. Piao H, Kwon J-S, Piao S, Sohn J-H, Lee Y-S, Bae J-W, Hwang K-K. Effects of cardiac patches engineered with bone marrow-derived mononuclear cells and PGCL scaffolds in a rat myocardial infarction model. *Biomaterials.* 2007;28(4):641-649.

41. Wei H, Chen S, Chang Y, Hwang S, Lin W, Lai P, Chiang H, Hsu L, Yang H, Sung H. Porous acellular bovine pericardia seeded with mesenchymal stem cells as a patch to repair a myocardial defect in a syngeneic rat model. *Biomaterials.* 2006;27(31):5409-5419.

42. Kofidis T, Akhyari P, Wachsmann B, Boublik J, Mueller-Stahl K, Leyh R, Fischer S, Haverich A. A novel bioartificial myocardial tissue and its prospective use in cardiac surgery. *Eur J Cardiothorac Surg.* 2002;22(2):238-243.

43. Infanger M, Faramarzi S, Grosse J, Kurth E, Ulbrich C, Bauer J, Wehland M, Kreutz R, Kossmehl P, Paul M, Grimm D. Expression of vascular endothelial growth factor and receptor tyrosine kinases in cardiac ischemia/reperfusion injury. *Cardiovasc Pathol.* 2007;16(5):291-299.

44. Umar S, Hessel M, Steendijk P, Bax W, Schutte C, Schalij M, van der Wall E, Atsma D, van der Laarse A. Activation of signaling molecules and matrix metalloproteinases in right ventricular myocardium of rats with pulmonary hypertension. *Pathol Res Pract.* 2007;203(12):863-872.

45. Tammela T, Enholm B, Alitalo K, Paavonen K. The biology of vascular endothelial growth factors. *Cardiovasc Res.* 2005;65(3):550-563.

Appendix A: LabVIEW Program

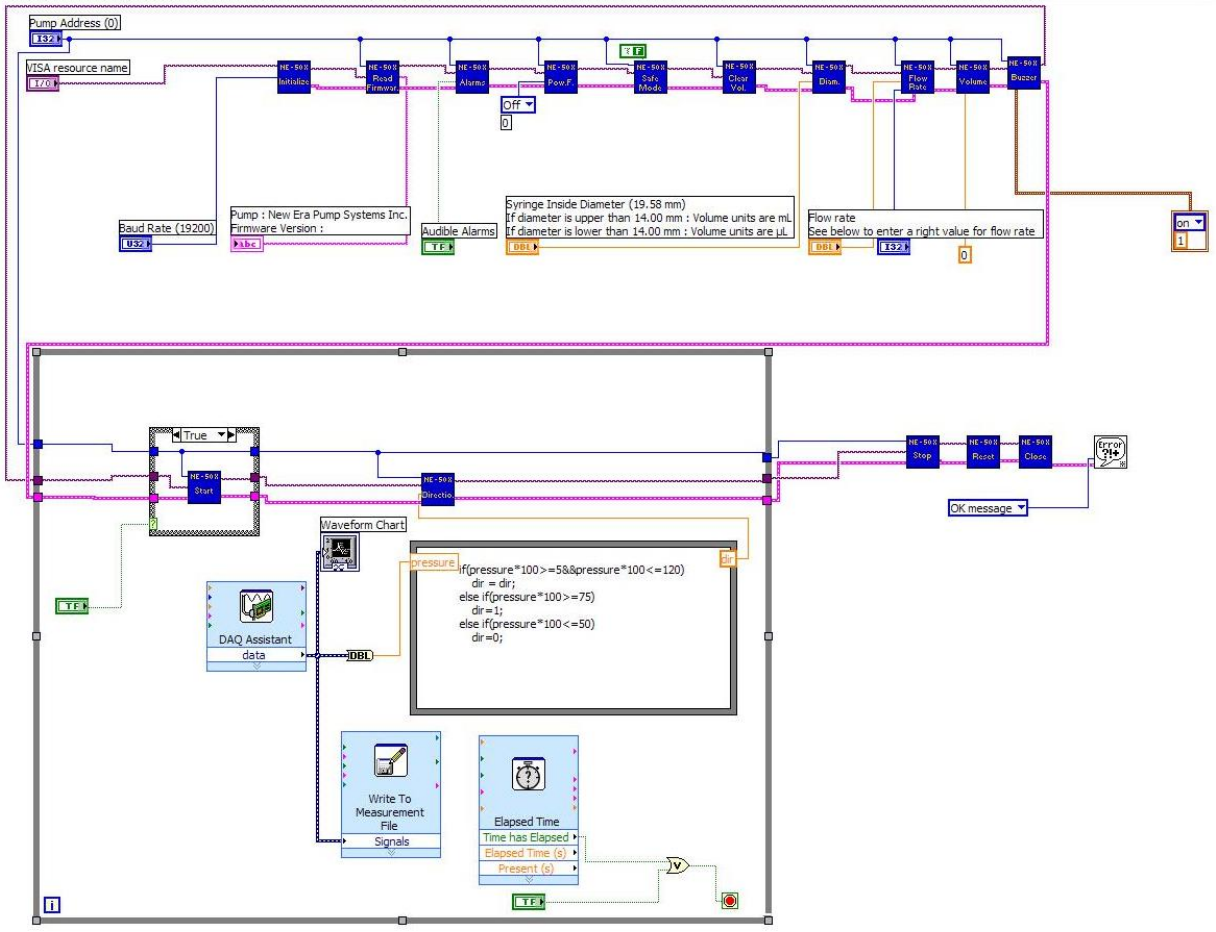
Pump Address (0)
VISA resource name
Baud Rate (19200)
Pump : New Era Pump Systems Inc.
Firmware Version :
Audible Alarms
Syringe Inside Diameter (19.58 mm)
If diameter is upper than 14.00 mm : Volume units are mL
If diameter is lower than 14.00 mm : Volume units are µL
Flow rate
See below to enter a right value for flow rate
Off
True
Waveform Chart
DAQ Assistant
data
pressure
dir
if(pressure*100>=5&&pressure*100<=120)
dir = dir;
else if(pressure*100>=75)
dir=1;
else if(pressure*100<=50)
dir=0;
Write To Measurement File
Signals
Elapsed Time
Time has Elapsed
Elapsed Time (s)
Present (s)
OK message

Appendix B: Sonomicrometry User Manual

Fundamental Theory

Background

Sonomicrometry, as applied to biomedical research, is the measurement of distances within soft tissue by using sound energy. Small piezoelectric crystals perform the task of transmitting and receiving short pulses of ultrasonic energy. These crystals are embedded, sutured, or otherwise fixed to the endpoints of the distances to be measured.

As illustrated in Figure 1, for a single distance measurement, one crystal is electrically energized causing an oscillatory shape change, which results in a burst of sound typically several hundred kHz or a few MHz in frequency. This process is not unlike a hammer hitting a bell. Depending on the shape of the crystal, this sound wave can travel in a narrow beam, or it can radiate in many directions. Eventually, this sound wave will impinge on a second crystal, causing it to produce a weak electrical current in response to the sound-pressure energy emitted by the first crystal.

It is the ***"time of flight"*** of the sound wave as it travels between the transmitting and receiving crystals that is actually measured in sonomicrometry. Since the speed of sound in soft tissue is well characterized, a simple calculation (Distance = Velocity x Time) yields the distance between the crystals.

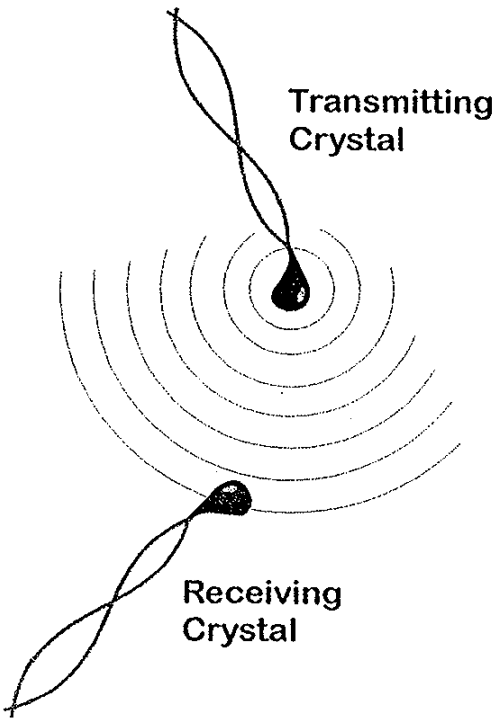

Figure 1 Ultrasonic Transmission and Reception Using Piezoelectric Transducers.

If two, or more, crystals are used as receivers, then a simultaneous distance measurement between the transmitting crystal and ***all*** receiving crystals can be made. In addition, it is possible to alter the function of some or all of the crystals so that they are capable of both transmitting and receiving. These crystals are called ***transceivers.*** The advantage of having a group of crystals acting as transceivers is that all possible distance measurements between crystals can be obtained.

Typically, 2 to 32 crystals are implanted during an experiment. During operation, the computer rapidly switches these crystals between transmit and receive modes, thus allowing the user to obtain measurements between any of the implanted crystals. The delay between successive measurements is usually small enough to be considered insignificant when compared to biological motion.

Conventional Systems vs. the Digital Sonomicrometer

Conventional sonomicrometers use analog circuitry that is decades old. The elapsed time between transmit and receive signals is measured using an analog capacitive charging circuit, and the voltage that represents the measured distance must be output to a strip recorder in analog form. This data must then be somehow digitized for computer analysis. Distances are always measured between dedicated transmitters and receivers, and each additional distance that is measured requires an additional channel to be added to the main unit (Figure 2). This required 2 x N crystals for N distances. Eight distances would therefore require an 8 Channel Unit (each channel consisting of one receiver and one transmitter) with 16 crystals.

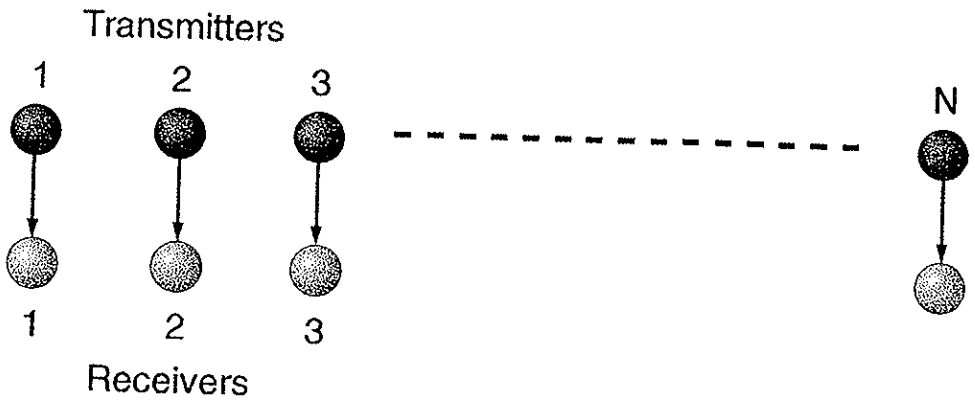

Figure 2 Conventional systems require an additional pair of crystals for every additional distance

The Sonometrics' Digital Sonomicrometer can receive from any transmitter and can also transmit from any crystal, therefore, dramatically reducing the number of crystals and independent channels that you need to get the measurements you require.

Each crystal is automatically configured as a transmitter for one firing cycle, and then reconfigured as a receiver for the subsequent firing cycles. With this system, you can measure all the distances between an array of crystals, thus establishing a set of coordinates for 3-D reconstruction (see 3D Coordinate Software). The number of unique distances that can be measured is defined by the equation:

$$\#\text{ of Distances} = \binom{N}{2} = \frac{N!}{2!(N-2)}$$

Where N is the number of crystals present in the array.

With 8 crystals, a total of 28 unique distances can be measured. With 16 crystals, 120 unique distances can be measured. As can be seen from Figure 3, some of the distances are measured twice, which is why only the unique distances are counted. In reality, the Digital Sonomicrometer measures N^2 distances in each firing cycle. A 16-crystal system, therefore, measures 256 distances, half of them being copies of the others. This redundant measurement can often be a good method for verifying the accuracy of the transceiver pair.

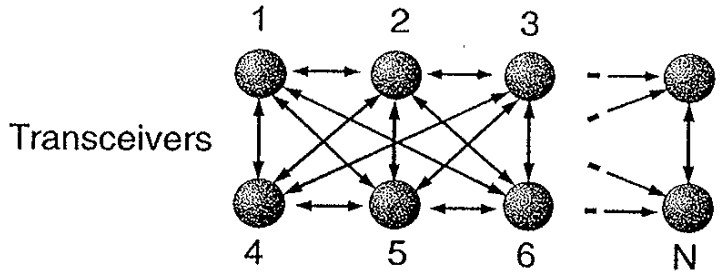

Figure 3 The Digital Sonomicrometer can measure distances between an array of crystals, when connected to transceivers.

The Sonometrics Digital Sonomicrometer

The determination of distances using sonomicrometry involves the measurement of the elapsed "time of flight" of sound between transmitting and receiving crystals. This is accomplished by the use of a digital counter that operates at a frequency of 64 MHz (or 100 MHz for a higher resolution), which provides a resolution of 24 μm (or 15 μm).

During the activation of a transmitting crystal, a ***transmit pulse*** signal is used to apply a high potential to the crystal, causing it to oscillate. Variations in the duration of the transmit pulse signal can cause a considerable change in the strength of the resulting transmitted sound wave. The length of the transmit pulse signal is under user control, and can be changed while observing the effects on the signal strength and distance measurements. The transmit pulse length ranges from 31 ns to 2 ms in 31 ns increments.

At the instant that a transmitting crystal is activated, all digital distance counters are reset to zero, and then they begin to increment at a rate of 64 MHz (or 100 MHz). The instant that the receiving crystals receive the burst of transmitted ultrasound, their respective digital counters are halted and the resulting numbers are transferred directly to a RAM memory buffer. Thus, there is no analog conversion process involved in these time measurements, which eliminates the need to calibrate the system.

The circuitry in the Sonometrics Sonomicrometer allows for up to 32 such distance measurements to be performed simultaneously. The counters that perform the distance measurements are 14 bits wide, allowing for a maximum measurable distance of 400 mm at 64MHz. In actual use, the range of measurement is software limited from 0 - 196 mm.

The practical range of measurement depends a great deal on the type and shape of the crystals used, but the typical range is from 10 mm to 120 mm. The smallest measurable change in distance at 64 MHz operation is 0.024 mm, (0.015mm resolution at 100 MHz) and this is linear throughout the entire measurement range.

A characteristic of sonomicrometry is that the receiving crystals and receiving circuitry are susceptible to the transmit signal that activates the transmitting crystals. This susceptibility takes on the form of a burst of noise that starts at the instant the transmitting crystal is activated and can last for up to 2 μs. During this time, the receiving circuitry is unable to process any signals from the receiving crystals. This is known as the ***inhibit time***, because the signals from the receiving circuits to the digital distance counters must be "inhibited", or they would have the effect of stopping the distance counters prematurely. The inhibit time has the same range as the digital distance counters, and is software adjustable in steps of 0.1μs. (NOTE:

This time measurement is converted to a distance in the SonoLAB software. You will notice that it is named *inhibit delay*, and is adjustable in 0.1 mm increments.).

The transmitting and receiving circuitry is combined to form a transceiver. The Sonometrics Sonomicrometer can activate up to 32 crystals as transceivers. Digital circuitry automatically activates all transmitters in a pre-set sequence, and keeps track of the resulting digital count values. For example, in a system that has 16 transceivers, there is a total of 240 distance measurements (120 unique distance measurements performed twice).

The rate at which the circuitry cycles through the transmitters is determined by the ***cycle time,*** allotted to each transceiver. This sampling frequency is programmable from 28μs to 2044μs, in increments of 16 μs. At the end of each cycle, the data from the distance counters is transferred to a bank of on-board RAM memory. Then the next transceiver is activated and another measurement cycle is performed. When all transmitters have been activated in this manner, a complete ***block*** of measurements has been performed, and the circuitry automatically starts another block of measurements. The on-board memory has the capacity to store up to 512 such blocks of data.

In order to perform distance measurements of up to, for example, 150 mm, the cycle time must be at least 100 μs due to the transit time of sound across such a distance. In addition, more time might be needed to allow the acoustic energy to dissipate before the next measurement cycle is started. Thus, cycle times of 350 μs to 450 μs are not uncommon. The total time needed to perform a block of measurements is the product of the number of transmitters and the transmitter cycle time. If 16 crystals are operated as transmitters (or transceivers), and the cycle time is set to 350 μs, then the block time would be 5.6 ms, giving a total sampling frequency of 178 Hz.

A separate circuit board, which interfaces directly with the PC-AT bus inside the computer, performs the function of digitizing external analog signals from pressure transducers, flow probes, and EKG. Up to 16 channels of conversion is available. The conversion of these analog signals is performed simultaneously with virtually no phase shift, and occurs once per block of sonomicrometry measurements. Analog signals with a range of -10 volts to +10 volts are digitized to 12 bits (4096 discrete values) giving a resolution of 4.88 mV per value. The A/D controller board has its own RAM memory buffer, which enables the storage of up to 8192 samples per channel.

The SonoLAB data acquisition software can store up to 5000 blocks of data at rates exceeding 200 Hz without missing a single measurement sample because it maintains it's own data buffer in the computer's RAM. The data is transferred in a packed-binary format, at 12 bits per sample, to the computer's hard disk drive. During use, the user selects the active transceivers, analog channels, as well as transceiver cycle-length, transmit pulse-length, and inhibit time. These parameters, along with the time and date of data acquisition, are stored along with the raw data.

Sources of Error

The measurement of distance between two crystals has four possible sources of error:
The accuracy of the time measurement.
The addition or subtraction of an offset to the calculated distance.
Variations in the speed of sound.
The reception of the signal at the receiving crystal.

Since an extremely stable 64 MHz crystal oscillator is used as the time-base, the measurement of the ultrasound transit-time it is not a source of error. The addition, or subtraction, of an offset value to the calculated distance results from known system delay times, and somewhat, on the actual crystal geometry. The error in the offset value affects only the absolute distance measurement, not the measured changes in distance. The maximum error associated with this offset value is estimated to be 1.5 mm or less.

The received signal varies primarily in strength, and is the prime source of error. The profile of the received signals has been found to be independent of the type and geometry of the crystals that are commonly used. In general, the received ultrasonic signals consist of a number of cycles of a sine wave, the amplitude-envelope of which is elliptical shaped. That is, the signal strength builds over the course of the first several cycles, and typically reaches maximum strength by the third or fourth cycle.

The function of the detection circuitry in the receiver is to detect the presence of a received signal at the earliest possible moment. Ideally, it must be sensitive enough to discriminate the reception of the first cycle of the received signal, but it must reject any ambient noise that the receiving circuit may pick up. The receiver therefore employs a detection threshold that the received signal must cross. During situations of weak signal reception, the detection circuitry may alternate between detection of the first, second, or even third cycle of the received signal.

Since these cycles are periodic, there is a fixed time interval between them. This leads to a fixed jump, or ***level-shift***, in the measured distance. This level-shifting phenomenon, when present, is usually periodic with the motion of the crystals, which is related to the motion or shape-change of the organ being monitored.

Data Post-Processing: The SonoVIEW Program

An advantage of **digitally measuring**, and recording, every distance measurement is that, when a level-shift occurs, it is visually apparent. Other problems such as weak or defective crystals, electrical interference from other laboratory devices, or sonic interference from other ultrasound sources, may be present from time to time. This leads to single point outliers, and can be removed using automated signal processing algorithms such as SonoFILT. This is in contrast to older-style sonomicrometers, which, due to their analog output stage, have the effect of lengthening short-duration interference, which can be falsely interpreted as a real change in distance. This is especially true for level-shifts, in which case the magnitude of a contractile measurement can be over-estimated because of the presence of incorrect level-shifts.

Sonometrics provides **SonoVIEW** post-processing software that allows the user to visually examine each trace of data. Data processing operations such as removing data-outliers and level shifts can be performed according to a fixed set of algorithms. If the signals seem extraordinarily bad, then the user can filter the data through the use of **SonoFILT**, which is also provided. The end result of altering the data traces is to form a continuous distance function by selectively removing discontinuities. The discontinuities arise from interference picked up by the receiver, and from the level-shifting effect described above.

Once a data file has been examined and filtered by the SonoVIEW program, all distance and analog data is output to an ASCII-readable data file that allows for further data processing and graphing by other programs.

Three-Dimensional Triangulation of Sonomicrometer Data

From a mathematical standpoint, it is possible to calculate the three-dimensional coordinates of a set of points if the distances between those points are known. As applied to sonomicrometry, this process starts by selecting three crystals that form what is referred to as a reference plane. The reference plane is defined to have a z-axis value of zero, and the three reference crystals (Q1, Q2, and Q3) have the coordinates {x,y,z} of (0,0,0), (X1,0,0), and (X2,Y2,0) respectively.

Once a general solution for the coordinates of all crystals is known, an error-minimization algorithm can be employed. These algorithms essentially determine the "coordinate of best fit" based on all available distance data and the computed set of three-dimensional coordinates. This error function attempts to minimize the difference between the calculated distances between coordinates and the actual, original distance data. This process is repeated for each sampled point in time, so that a four-dimensional representation can be reconstructed.